

Investigating the role of *Pseudomonas syringae* pv. *tomato* biofilm formation during successful infections and the effect of PAMP-Triggered Immunity on biofilm formation in *Arabidopsis*

By Wantao Noah Xiao, BSc.

A Thesis Submitted to the School of Graduate Studies in Partial fulfillment of the Requirements for the Degree Master of Science

McMaster University © Copyright by Wantao Xiao, April 2021

McMaster University Master of Science (2021) Hamilton, Ontario (Biology)

Title: Investigating the role of *Pseudomonas syringae* pv. *tomato* biofilm formation during successful infection and the effect of PAMP-Triggered Immunity on biofilm formation in *Arabidopsis*

Author: Wantao N. Xiao, B.Sc. (McMaster University)

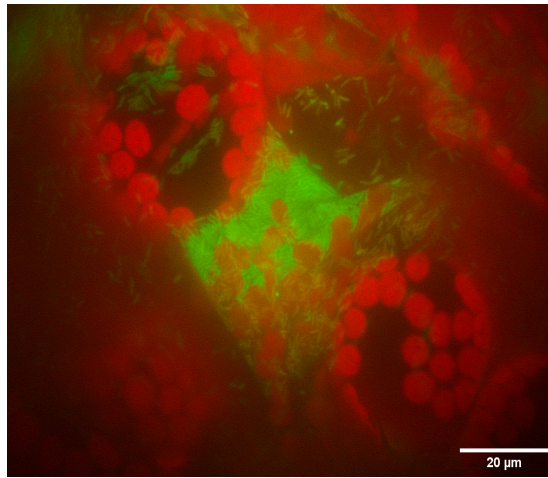
Supervisor: Dr. Robin K. Cameron

Number of pages: ii-xiv; 1-102

Abstract

Plants rely on innate immunity to perceive and respond to pathogenic microbes. Pathogenic microbes suppress and evade plant immune responses to obtain nutrients and multiply resulting in plant diseases and death. One battleground for the arms race between plants and microbial invaders is located in the leaf intercellular space, specifically between *Pseudomonas* bacteria and *Arabidopsis*. This thesis seeks to understand the virulence mechanisms that allow *Pseudomonas* bacteria to grow within the leaves of *Arabidopsis* and how the plant immune response reduces pathogen growth and reproduction. Some plant pathogens produce specific extracellular polysaccharides to potentially enhance pathogenicity during infection of plants. The objective of this thesis is to understand the importance of biofilms for *Pseudomonas* success and determine if *Arabidopsis* suppresses biofilm formation as part of the plant immune response. It was hypothesized that biofilm formation contributes to *Pseudomonas* success *in planta* and *Arabidopsis* suppresses biofilm formation during PAMP-Triggered Immunity (PTI) to reduce bacterial growth. Wild-type plants and defense mutants were infiltrated with flg22 or mock (water) treatments to induce or mock-induce PTI in plants, followed by observing GFP-expressing *Pseudomonas* via fluorescence microscopy to determine if biofilm-like aggregate formation was occurring. *In vivo* studies in this thesis indicate that biofilm-like aggregate formation contributes to bacterial success during *Arabidopsis* infection. Additionally, the phytohormone, salicylic acid (SA), accumulates in leaf

intercellular spaces of resistant plants during PTI that suppresses biofilm formation, suggesting that SA acts as an anti-microbial and anti-biofilm agent that contributes to the suppression of pathogen growth during plant defense.



GFP-expressing aggregated *Pseudomonas* in the intercellular space of an *Arabidopsis* leaf

Acknowledgments

I want to express my sincere appreciation to my supervisor, Dr. Robin Cameron, for being an amazing mentor. You have played such important role in my life helping me grow from a teenager into a passionate and confident young scientist and also a kind caring adult. I am forever grateful for your acceptance when everyone had said no. You discovered my talents and nourished my passion for plant research into a life-long career. No matter what I may do and no matter where I may be in the future, I will always feel proud of being your pupil. I also want to express my gratitude for my committee members, Dr. Rosa Da Silva and Dr. Weretilnyk, for your patience, guidance and also for giving me so much advice and resource for my study. To Angela who has become one of my favorite people in the whole world, you are my best friend, big sister, and the person I look up to the most. You are so inspiring and so wise on so many levels. I may never be able to find another lab partner like you and I am so happy for being your partner in crime during our time together! This project would never have come this far without the huge contribution from everyone in the lab, especially Natalie, Garrett, Tenzin and Abdul. Thank you for doing so much as part of the team. Lastly, I want to express my appreciation to everyone who has showed me kindness during my 6 years at McMaster University. To Mihaela, Alastair, Alison, Susan, JP, Kathy, Barb, Arlene, Julie, Scott and Tracy, thank you for your friendship, advice, help and everything you have done for me during these years. All of you have gave me support and kindness when I felt hopeless, helpless and

lonely. I am forever grateful for the time we spent together, and I will come back every spring to visit everyone with flowers! To my pal Albert, I always feel we have been friends for years even though it has only been two years. Thank you for all the help with editing. I know you are a true friend when you said you are happy to look at all my writing scraps and helped me to turn them into something great! I also want to thank my family. I want to thank my parents for supporting my studies and a comfortable life in a foreign country. Even though I have not seen my mother for 5 years and my dad for 6 years in person, my connection with my family has never faded. I want to thank Michael for being a supportive and loving partner who keeps me happy and content during a crazy time of life, even though you drive me crazy sometimes. Special thanks for my loving golden retriever Kinomi, I would not be able to do what I do without knowing you and Mike are waiting for me at the end of day. I hope that what I have accomplished so far makes everyone who cares about me, truly proud!

Table of Contents

Abstract.....	iii
Acknowledgements.....	v
Table of Contents.....	vii
List of Figures.....	x
List of Tables.....	x
List of Abbreviations.....	xi
Declaration of Academic Achievement.....	xiv
Chapter 1: introduction	
1.1 Plant responses to the environment.....	1
1.2 Plant responses to plant pathogens.....	1
1.2.1 The <i>Arabidopsis thaliana</i> - <i>Pseudomonas syringae</i> pathosystem.....	2
1.2.2 PAMP-Triggered Immunity (PTI)	3
1.2.2.1 Flagellin & FLS2 in <i>Arabidopsis thaliana</i>	4
1.2.2.2 Salicylic acid defense signaling during PTI.....	5
1.2.3 Intercellular SA accumulation contributes to ARR as an antimicrobial.....	7
1.2.4 Effector-Triggered Susceptibility.....	10
1.3 Plant-associated Bacterial Biofilms.....	12
1.3.1 Biofilm matrix components.....	18
1.3.1.1 Alginate in Bacterial Biofilms.....	20
1.3.1.2 Alginate Biosynthesis.....	22
1.3.1.3 AlgD.....	23

1.3.1.4 AlgU.....	24
1.4 Intercellular SA accumulation contributes to ARR as an antibiofilm agent.....	25
1.5 Hypotheses and Objectives.....	26
Chapter 2: Materials and Methods	
2.1 <i>Arabidopsis</i> plant lines and growth conditions.....	27
2.2 Bacterial strains and transformation.....	28
2.3 disease resistance assay.....	29
2.4 Imaging of <i>Pst</i> in the intercellular space by fluorescence microscopy.....	29
2.5 Biofilm Matrix staining.....	30
2.6 Intercellular washing fluid (IWF) collection.....	32
2.7 Biosensor SA quantification.....	32
2.8 Statistical tests.....	33
Chapter 3 Investigating biofilm formation by <i>Pseudomonas syringae</i> pv. <i>tomato</i> and the effect of PAMP-Triggered Immunity on biofilm formation in <i>Arabidopsis</i>	
3.1 Preface.....	34
3.2 Author contributions.....	34
3.3 Bacterial aggregate formation is associated with successful infection by <i>Pst</i> ..	35
3.4 The PTI response is associated with reduced bacterial aggregate formation..	38
3.5 Visualization of the <i>Pst</i> extracellular matrix.....	40
3.6 The ability to produce alginate is not required for <i>Pst</i> success <i>in planta</i> but contributes to <i>Pst</i> aggregate formation.....	42

3.7 Effect of plant-produced SA on <i>Pst</i> and <i>Pst</i> $\Delta algD$ aggregate formation and size.....	45
3.8 Bacterial pathogenicity is associated with the ability to form aggregates....	48
3.9 Effect of plant-produced SA on <i>Pst</i> $\Delta algD$ $\Delta algU$ $\Delta mucAB$ aggregate formation and size.....	49
3.10 Early SA accumulation contributes to suppression of bacteria biofilm formation.....	54
Chapter 4: Discussion and Conclusions	
4.1 <i>Pst</i> biofilm formation visualization.....	57
4.2 Functional alginate biosynthesis is important for biofilm-like aggregate formation, but not for growth of virulent <i>Pst</i> in <i>Arabidopsis</i>	60
4.3 Biofilm-like aggregate formation contributes to <i>Pst</i> pathogenicity.....	64
4.4 PTI suppresses biofilm-like aggregate formation & bacterial success in a SA-dependent manner <i>in vivo</i>	69
4.5 During PTI SA accumulates in leaf intercellular spaces and is associated with suppression of <i>Pst</i> growth and biofilm-like aggregate formation <i>in vivo</i>	71
4.6 Conclusions and novel contributions to knowledge.....	73
4.7 Future directions.....	74
Appendix A	78
References	80

List of figures

Figure 1. Visualization of GFP-expressing <i>Pst</i> in susceptible and PTI-responding leaves.....	36
Figure 2. Visualization of the <i>Pst</i> extracellular matrix.....	41
Figure 3. Growth and aggregate formation of <i>Pst</i> and <i>Pst</i> $\Delta algD$ in Col-0 and <i>sid2-2</i>	44
Figure 4. Quantification of aggregate size and number in <i>Pst</i> & <i>Pst</i> $\Delta algD$ in wild-type Col-0 and <i>sid2-2</i>	47
Figure 5. Growth and aggregate formation of <i>Pst</i> & <i>Pst</i> $\Delta algD\Delta algU\Delta mucAB$ in wild-type Col-0 and <i>sid2-2</i>	49
Figure 6. Quantification of aggregate size and number in <i>Pst</i> & <i>Pst</i> $\Delta algD\Delta algU\Delta mucAB$ in wild-type Col-0 and <i>sid2-2</i>	53
Figure 7. SA accumulation in intracellular washing fluids during PTI.....	56
Figure A1. PTI RNA Quality Check Analysis.....	78

List of Tables

Table 1. PTI response varies across experiments.....	37
Table 2. Percent FOV with <i>Pst</i> aggregates in flg22- and mock-treated leaves....	38
Table A1. PTI response suppresses bacterial levels <i>in planta</i>	79

List of Abbreviations

μl	microliter
μm	micrometer
μM	micromolar
AlgD	GDP-mannose 6-dehydrogenase
AlgU	RNA polymerase sigma-H factor
ANOVA	Analysis of variance
ARR	Age-related resistance
Ca^{2+}	Calcium ion
cfu	colony forming units
Col-0	Columbia-0
ConA	Concanavalin A
COR	Coronatine
DAPI	4',6-diamidino-2-phenylindole
eDNA	extracellular DNA
EPS	Extracellular polymeric substances
ETI	Effector-triggered immunity
ETS	Effector-triggered susceptibility
FLS2	Flagellin sensing 2
Flg22	Flagellin 22
FOV	Field of view
GFP	Green fluorescent protein

HIM	Hrp-inducing minimal medium
hpi	hours post-inoculation
HR	Hypersensitive response
Hrp	Hypersensitive response and pathogenicity
HSD	Honestly significant difference
ICS1	Iscochorismate synthase 1
JA	Jasmonic acid
ld	leaf disc
LPS	Lipopolysaccharide
LRR	Leucine rich repeat
MgCl ₂	Magnesium chloride
MucA	Sigma factor AlgU negative regulatory protein A
MucB	Sigma factor AlgU negative regulatory protein B
ml	milliliter
mM	millimolar
nm	nanometers
NPR1	Nonexpressor of PR genes 1
PAMP	Pathogen-Associated Molecular Pattern
PR	Pathogenesis-Related Proteins
PRR	Pattern recognition receptor
<i>Psg</i>	<i>Pseudomonas syringae</i> pv. <i>glycinea</i>
<i>Pss</i>	<i>Pseudomonas syringae</i> pv. <i>syringae</i>

<i>Pst</i>	<i>Pseudomonas syringae</i> pv. <i>tomato</i>
<i>Pta</i>	<i>P. syringae</i> pv. <i>tabaci</i>
PTI	Pattern-triggered immunity
RLK	Receptor-like kinases
ROS	Reactive oxygen species
SA	Salicylic acid
SID2	Salicylic acid induction deficient
T3SS	Type III Secretion System

Declaration of Academic Achievement

This thesis was written by Wantao (Noah) Xiao with the help and guidance from Dr. Robin K. Cameron. The project was conceived of and developed by Robin Cameron, Angela Fufeng, and myself. Experiments characterizing biofilm-like aggregate formation and bacterial success of *Pst in planta* were mostly carried out by Angela Fufeng and myself. I then performed aggregate size analysis. The biofilm component staining protocol was developed for use in our lab by Abdul Halim, myself and Robin Cameron. The biofilm component staining experiments were carried out by Abdul and myself. Experiments involving Intercellular washing fluid collection were performed by Garrett Nunn, Natalie Belu, Tenzin Gyaltzen, Abdul Halim and myself. I performed all salicylic acid biosensor assays to determine leaf intercellular SA levels.

I declare this thesis to be an original report of our research, except where indicated by referencing. No part of this work has been submitted, in whole or in part, in any previous application or publications for a degree at another institution. All research conducted in this thesis will be prepared for a manuscript submission to a peer-reviewed journal. The first draft of the manuscript will be written by Wantao (Noah) Xiao as first author and edited by Dr. Robin Cameron as corresponding author. Angela Fufeng (second author), Garrett Nunn (third author), Abdul Halim (fourth author) and Natalie Belu (fifth author) will also contribute editorial efforts to completion of the final manuscript.

Chapter 1: Introduction

1.1 Plant responses to the environment

Plants make up more than 80% of the biomass on earth. They serve as a food source and provide shelter and oxygen for microbes and animals (Bolund and Hunhammar 1999). However, plants are immobile and cannot move to escape from environmental stress. For this reason, plants experience many environmental stresses differently from animals, in terms of both abiotic (water, nutrient, light and temperature extremes) and biotic stress (competition with other plants, predation by herbivores and infection by pathogens). Therefore, plants evolved sophisticated signaling pathways and defense mechanisms to detect and respond to various internal and external conditions.

1.2 Plant Responses to Plant Pathogens

The ongoing evolutionary arms race between microbial pathogens and plants has given rise to a complicated relationship between plants and microbes (Jones and Dangl 2006). Pathogens such as fungi, bacteria and viruses have evolved complex mechanisms to invade plants and evade plant immunity/defenses. Meanwhile, plants have evolved defense responses to counteract pathogen infection and protect themselves from microbial diseases. Thus, detection of and defense against pathogens are important for plant survival. As a result, defense signaling pathways are conserved across many plant species (Jones and Dangl 2006). Constitutive defenses such as cell walls, waxy epidermal cuticles, and bark act as barriers to many pathogen infections (Jones and Dangl 2006).

Constitutive defenses can be breached by some pathogens allowing invasion of plant tissues, however, local plant responses are initiated as the first line of induced defense. This includes a number of different defense responses including Pathogen-Associated-Molecular-Pattern (PAMP)-Triggered Immunity (PTI). The *Arabidopsis thaliana*-*Pseudomonas syringae* plant-microbe pathosystem is a popular model pathosystem used by many plant biologists in the world to study plant immune responses like PTI.

1.2.1 The *Arabidopsis thaliana*-*Pseudomonas syringae* pathosystem

The gram-negative bacterium *P. syringae* is a common plant pathogen, infecting a wide range of commercial crops (Arnold and Preston 2019). For instance, the kiwifruit is one of New Zealand's most economically valuable exports and the kiwifruit industry suffered a catastrophic outbreak of *P. syringae* pv. *actinidiae* and lost billions of dollars in 2007 (Renzi, Mazzaglia, and Balestra 2012). To develop a model system for molecular genetic analysis of plant-pathogen interactions, Whalen et al. (1991) and Dong et al. (1991) developed *Arabidopsis*-*P. syringae* systems and published their studies in the same year. This led to the world-wide application of the *A. thaliana*-*P. syringae* pathosystem for research in plant-pathogen interactions. This model pathosystem has significantly contributed to the scientific community's understanding of pathogen infections and plant resistance (Katagiri, Thilmony, and Yang 2002).

P. syringae mainly infects the aboveground organs of plants such as leaves. The disease cycle was summarized by Xin and He (2013) and begins with an

epiphytic growth phase in which bacterial cells survive on the leaf surface and then enter the intercellular space via stomata. Once inside a susceptible host leaf, *P. syringae* can multiply quickly in the intercellular space and cause disease symptoms like chlorosis. *P. syringae* feeds on nutrients from living host cells during early stages of the infection (biotrophy), and from dead cells during later stages (necrotrophy). During the necrotrophic phase, *P. syringae* produces enzymes to break down plant cell walls resulting in host cell death causing necrotic spots on the leaves providing nutrients and access to the leaf surface for dispersal (Choi et al. 2013; Kubicek, Starr, and Glass 2014; Xin and He 2013). Therefore *P. syringae* is classified as a hemi-biotroph (Glazebrook 2005; Xin and He 2013). This thesis involves examinations of pathogenicity (defined as the capability of a pathogen to cause diseases) and virulence (defined as the degree of pathogenicity of a given pathogen) of *P. syringae* (Agrios 2005). When a subgroup of *P. syringae* strains can only infect plants within a certain genus or species, the subgroup is defined as a pathovar of *P. syringae* (Agrios 2005). Although many concepts mentioned in this thesis may be applicable to other plant-pathogen interactions, the information given in subsequent sections pertains to the *A. thaliana*-*P. syringae* pathosystem unless otherwise indicated.

1.2.2 PAMP-Triggered Immunity (PTI)

PTI begins with the perception of PAMPs (Pathogen-Associated Molecular Patterns) by immune receptors found on the plant plasma membrane. PAMPs are essential molecular components for bacterial survival, and they are usually

highly conserved within microbe classes. (Zipfel 2009). These include flagella, and pathogen-specific liposaccharides in bacterial or fungal membranes that can be perceived by plant pattern recognition receptors (PRRs) to initiate a downstream signaling cascade resulting in expression of PTI-related genes. The PTI response includes the closure of stomata, production of antimicrobial compounds and pathogenesis-related (PR) proteins, and callose deposition to reinforce the cell wall (Geng *et al.* 2012; Zheng *et al.* 2012; Zheng *et al.* 2015), all of which contribute to the suppression of bacterial growth and disease (Zipfel 2009; Hann and Rathjen 2007).

1.2.2.1 Flagellin and FLS2 in *Arabidopsis thaliana*

Arabidopsis thaliana recognizes a wide range of bacterial PAMPs, some of which are derived from the structural components of the bacterial cell (Zipfel 2009). Although many bacterial PAMPs have been identified, few PRRs have been discovered (Bigear, Colcombet, and Hirt 2015b). The most studied PRR-PAMP interaction is between the bacterial flagellin peptide flg22 and the plant PRR, FLAGELLIN SENSITIVE 2 (FLS2) (Jelenska *et al.* 2017). The flagellin protein is recognized by most plants and is the building block of bacterial flagella. (Boller and Felix 2009). The peptide flg22, corresponds to 22 amino acids localized in the conserved region of some bacterial flagella including *Pseudomonas syringae*. (Jelenska *et al.* 2017). The PRR FLS2 is a leucine-rich repeat receptor kinase with an extracellular domain, a transmembrane domain, and a cytoplasmic serine/threonine kinase domain (Gómez-Gómez and Boller

2000). *Arabidopsis* FLS2 binds directly to flg22 and is responsible for recognition specificity based on *in vitro* data (Chinchilla et al. 2006). In wild-type *Arabidopsis* (Col-0 ecotype), treatment of leaves with solutions of flg22 initiates PTI and limits the growth of pathogenic *Pseudomonas syringae* pathovar (pv.) *tomato* (*Pst*) (Aslam et al. 2008).

1.2.2.2 Salicylic acid defense signaling during PTI

Salicylic acid (SA) is a major phytohormone involved in PTI signaling in response to biotrophic or hemibiotrophic infections (Glazebrook 2005). In *Arabidopsis*, upon perception of a PAMP (e.g. flg22), early PTI signaling events are initiated in plant cells and include calcium ion fluxes, production of ROS, and the activation of MAPK cascades (Taj et al. 2010; Faulkner and Robatzek 2012; Sinha et al. 2011; Zipfel 2009). As a result of these early signaling events, isochorismate synthase one (ICS1) located in the chloroplasts is expressed to catalyze the conversion of chorismate to isochorismate mainly via ICS1 (Zheng et al. 2015). Isochorismate is thought to be subsequently converted to SA by a hypothetical isochorismate pyruvate lyase (IPL) to produce SA in plants (Dempsey et al. 2011). However, some bacteria (such as *Escherichia coli*) employ an IPL that catalyzes isochorismate into pyruvate and SA (Ozenbergert, Brickman, and McIntosh 1989), but a recent paper indicated that *Arabidopsis* does not contain an IPL ortholog (Torrens-spence et al. 2019). Instead, Torrens-Spence et al. (2019) found that *AvrPphB* Susceptible 3 (PBS3) is important not only for SA accumulation but also for *in vitro* and *in vivo* production of an SA

biosynthetic intermediate, isochorismoyl-glutamate A. In addition, Torrens-Spence et al. (2019) identified Enhanced Pseudomonas Susceptibility 1 (EPS1) and demonstrated that it converts isochorismoyl-glutamate A to SA, which completes the chorismate SA biosynthesis pathway in *Arabidopsis*. Both metabolomic analysis of *Arabidopsis* mutants and *in vitro* enzymatic function analysis indicate that SA is produced via isochorismoyl-glutamate A, and also provides compelling evidence that PBS3 and EPS1 are the missing enzymes for SA biosynthesis in *Arabidopsis* (Torrens-spence et al. 2019).

Since SA biosynthesis is required in pathogen defense signaling in plants, SA biosynthesis *Arabidopsis* mutants involving these genes (e.g., *SID2*, *PBS3* and *EPS1*) support higher bacterial levels *in planta* and display greater symptoms (yellowing leaves) compared to wildtype *Arabidopsis* inoculated with virulent *P. syringae* (Torrens-spence et al. 2019). This is consistent with many previous findings that SA accumulation is important for plant-pathogen defenses such as PTI (Bigeard, Colcombet, and Hirt 2015b). For example, Tsuda and his team (2008) infiltrated four-week-old *Arabidopsis* Col-0 plants with 10 μ M flg22 solution to induce PTI and found that SA levels began to rise in leaves starting at 3 to 6 hours after flg22 treatment, with peak accumulation around 9 hours after flg22 treatment. The SA-deficient mutant *sid2-2* (*ics1* mutant) failed to accumulate SA after flg22 treatment and supported higher bacterial levels compared to wild-type *Arabidopsis* in infection assays (Tsuda et al. 2008). These data indicate the importance of SA accumulation for successful PTI responses in *Arabidopsis*.

When studying SA accumulation in plant defenses like PTI, researchers predominantly focus on the signaling pathways of SA in plants. Local defense signaling of SA accumulation in cells leads to production of PR proteins, and in some cases PR proteins have been shown to have antimicrobial activity (Carr, Beacw, and Klessig 1989). *PR1*, *PR2*, and *PR5* are expressed in a SA-dependent manner and have been shown to contribute to defense against the biotrophic fungus *Peronospora parasitica* in peas (Curto et al. 2006). In order to initiate defense gene expression such as *PR* genes, SA interacts with the co-regulator NPR1 in *Arabidopsis*, as demonstrated by experiments with *npr1* mutants that are defective in SA-dependent gene expression (Cao et al 1997). In the nucleus, NPR1 interacts with TGA transcription factors to promote expression of *PR* genes, resulting in local and systemic resistance (Zhang et al. 2003). Specific gene targets of NPR1 were discovered by Wang et al. (2005), who identified the NPR1-dependent upregulation of defense-associated PR genes and components of the secretory pathway, which likely facilitates the secretion of these proteins to the apoplast.

1.2.3 Intercellular SA accumulation contributes to ARR as an antimicrobial.

In addition to the signaling role of SA during defense responses, there is also evidence suggesting that SA may directly affect pathogen infection during plant responses such as ARR. ARR is a phenomenon in which mature plants display enhanced resistance to pathogens compared to young plants (Carviel et al. 2009). Resistant mature plants responding to *Pst* accumulated higher SA levels

in intercellular washing fluids (IWFs) extracted from the leaf intercellular space compared to young plants, suggesting that intercellular SA accumulation is important for ARR (Cameron and Zaton 2004; Carviel et al. 2014; Wilson et al. 2017). Since *P. syringae* is an intercellular pathogenic bacterium, intercellular accumulation of SA may directly act against *P. syringae* instead of as a signal during ARR. Many mutant and transgenic plants (*sid2-2*, *eds5-3*, *eds1-1*, *pad4-1* and *NahG*) are unable to accumulate SA and were demonstrated to be ARR-defective (Kus et al. 2002; Carviel et al. 2009; Wilson et al. 2017; Cameron and Zaton 2004), which suggests that SA is required for ARR. Furthermore, intercellular washing fluids collected from mature ARR-competent plants were observed to inhibit *Pst* growth *in vitro*, indicating the accumulation of antimicrobials (likely SA) in leaf intercellular spaces during ARR. (Cameron and Zaton 2004). When SA was infiltrated into leaf intercellular spaces, SA partially rescued the *iap1-1 Arabidopsis* (ARR defective mutant) and remain detectable in the intercellular space at 5h post-infiltration (Carviel et al. 2009). Furthermore, SA infiltration into intercellular spaces further enhanced ARR in Col-0 wild-type plants but only when SA was still present in leaf intercellular spaces, suggesting that SA acts as antimicrobial agent during ARR in leaf intercellular spaces and also suggesting that the role of SA may not involve signaling during ARR (Carviel et al. 2009). The non-signaling role of SA was further supported by evidence that young plants displayed high levels of *PR1* expression 12 to 24 hours after SA treatment, while mature ARR-responding plants expressed little *PR1* but

accumulated high levels of SA in leaf intercellular spaces (Cameron and Zaton 2004). Taken together, these data suggest that SA accumulates and acts an antibacterial compound in leaf intercellular spaces during ARR.

In addition to *in vivo* studies, multiple studies have shown that SA exhibits antimicrobial activity and is able to suppress phytopathogen growth *in vitro* (Amborabé et al. 2002; Brown, Swanson, and Allen 2007; Georgiou et al. 2000; Cameron and Zaton 2004). However, a range of concentrations were observed to have antimicrobial activity, likely due to varying experimental conditions and pathogens. A recent study in which *Pst* was incubated in *hrp*-inducing minimal (HIM) media supplemented with 100 to 200 μM SA demonstrated that SA had antibacterial activity against *Pst*. (Wilson et al. 2017). HIM media mimics the conditions of the intercellular space with a low pH of 5.7 (Jia and Davies 2007) and minimal nutrients, suggesting SA may have antimicrobial activities at similar concentrations *in planta*. In fact, concentrations of SA in leaf intercellular spaces were found to range from 40 to 100 μM in mature plants at 24 hours post *Pst* inoculation. These data suggest that SA may indeed act as an antimicrobial agent during ARR, especially given that intercellular SA may not be fully recovered during IWF collection and SA may also accumulate at higher concentrations in some microenvironments of leaf intercellular spaces. It has been suggested that a low pH may enhance the ability of SA to cross bacterial cell membranes, and this may be required for SA's antimicrobial activity (Amborabé et al. 2002). The mechanisms responsible for the antimicrobial

properties of SA during plant defense are not fully understood, but some studies suggest that SA may interfere with the microbial transmembrane proton gradient required for ATP production (Gutknecht 1990; Jörgensen et al. 1976; Norman et al. 2004), ultimately inhibiting respiration (Norman *et al.* 2004).

1.2.4 Effector-Triggered Susceptibility

In spite of sophisticated PTI signaling and responses, some pathogens overcome PTI with effector proteins (Jones and Dangl 2006). *P. syringae* delivers effectors into plant cells through the type III secretion system (T3SS). The most important T3SS structure is encoded by the *hrp/hrpC* locus made up of *hypersensitive reaction and pathogenicity (hrp)* genes because *hrp* genes contribute to *P. syringae* pathogenicity, which refers to the ability to cause disease and damage in the host (Cunnac, Lindeberg, and Collmer 2009). The T3SS consists of a secretion apparatus that delivers effector proteins across the inner membrane, the periplasmic space and outer membrane of bacteria, then across the plant cell wall and plasma membrane into the plant cell cytoplasm (Buttner and He 2009). In the *hrp/hrpC* locus of *P. syringae*, HrpA is the major component of the T3SS pilus which is required for effector secretion across the plant cell wall and plasma membrane (Boureau et al. 2002). Regulation of the locus involves HrpL as an alternative sigma factor that activates transcription of promoters for *hrp/hrpC* genes in *P. syringae* (Ortiz-martín et al. 2010). As effector proteins enter the host cells via the T3SS, the effector proteins manipulate host metabolism and suppress plant immune responses (Xin and He 2013). For

example, the AvrRpt2 effector protein found in *P. syringae* is a cysteine protease that cleaves RPM1-interacting protein 4 (RIN4) to release fragmented peptides that act as negative regulators of PTI (Afzal and Mackey 2011). However, many plants have also evolved counter measures to recognize effector proteins secreted by bacteria and induce a robust plant immune response called Effector Triggered Immunity (ETI) (Zhang and Zhou 2010). ETI is not the focus for this thesis so it will not be discussed further.

In addition to effector proteins that manipulate plant immune responses, some pathogenic *P. syringae* also secrete phytotoxins. For example, the phytotoxin coronatine is secreted by *Pst* and is involved in causing stomata to re-open after they close in response to PRR perception of PAMPs (Zheng et al. 2012). Additionally, coronatine interferes with the responses mediated by SA (Geng et al. 2012; Zheng et al. 2012; Ishiga et al. 2018; Block et al. 2005). Coronatine consists of coronafacic acid (CFA), which is an analog of methyl jasmonic acid (MeJA) and is able to activate the jasmonic acid (JA) pathway resulting in suppression of SA-dependent signaling and defense (Block et al. 2005). Binding of either JA or coronatine to the JA receptor triggers degradation of transcriptional repressors and thus relieves MYC2 (MYELOCYTOMATOSIS VIRAL ONCOGENE HOMOLOG2) suppression leading to upregulation of JA-responsive genes (Xin and He 2013; Geng et al. 2012). As a result of JA signaling, transcriptional factors are expressed that repress the SA biosynthesis gene *ICS1* and activate the SA metabolism gene *BSMT1* (*Benzoic Acid/Salicylic*

Acid Carboxyl Methyltransferase 1). JA signaling leads to a reduction in SA-mediated defense as the plant uses its resources to upregulate JA pathway genes to respond to insects and necrotrophic pathogens (Zheng et al. 2012). By secreting coronatine, *Pst* activates JA signaling to suppress SA accumulation and signaling to reduce plant defense and promote *Pst* success in the plant (Block et al. 2005).

1.3 Plant-associated Bacterial Biofilms

There is a growing body of evidence that the ability to form biofilms contributes to the pathogenicity and virulence of some bacterial and fungal pathogens. For example, biofilms are thought to protect bacteria such as *Pseudomonas aeruginosa* (a human pathogen) from environmental stresses like antimicrobial agents and antibiotics (Danhorn and Fuqua 2007). Bacterial biofilms are thought to consist of communities of surface-adherent aggregated cells embedded in a self-secreted matrix of extracellular polymeric substances (EPS) (Flemming and Wingender 2010). These communities may contain single or multiple species with properties that differ substantially from free-living planktonic bacterial cells (Flemming et al. 2016). The EPS matrix of bacterial biofilms is thought to contain bacterial proteins, lipids and extracellular DNA (eDNA) (Mann and Wozniak 2012). Biofilm formation is thought to occur in three main stages: (i) attachment to the device or cell surface, (ii) proliferation and formation of the characteristic mature biofilm structure, and finally (iii) detachment or dispersal of bacterial cells (Davey and Toole 2000). Attachment can occur passively in non-motile bacteria

such as Staphylococcal species or actively in motile bacteria such as *P. aeruginosa* (Joo and Otto 2012). Attachment is based on protein-protein interactions between the bacterial surface and host matrix proteins and maturation likely depends on adhesive factors such as exopolysaccharides, eDNA, and proteins (Joo and Otto 2012). Detachment occurs when cell to cell disruptive factors, such as surfactants, lead to the dispersal of bacterial cells (Davey and Toole 2000). Biofilms are also thought to provide bacteria with an increased capacity to resist antibiotic treatment and host-produced antimicrobial agents (Costerton, Stewart, and Greenberg 1999). *P. aeruginosa* biofilms were observed during an autopsy of the lungs of a cystic fibrosis patient who died from chronic *P. aeruginosa* infection (Hoiby, Ciofu, and Bjarnsholt 2010). It was shown that polymorphonuclear leukocytes surrounded, but did not penetrate into fluorescently labeled *P. aeruginosa* biofilm-like aggregates in an explanted lung of a cystic fibrosis patient with chronic lung infection (Hoiby, Ciofu, and Bjarnsholt 2010). Some leukocytes like neutrophils and macrophages engulf invading pathogens but it appears that these leukocytes were not able to engulf bacterial aggregates, suggesting aggregate formation provides protection for bacteria against human immune responses (Hoiby, Ciofu, and Bjarnsholt 2010). Altogether, it is believed that the *P. aeruginosa* biofilm matrix may be a barrier against antibiotics and leukocytes to protect bacteria from host immune responses (Rasamiravaka et al. 2015).

Bacterial biofilm formation in plant-bacteria associations has been studied in recent years (reviewed by Bogino et al. 2013 and Danhorn and Fuqua 2007). Plant-associated bacterial biofilms have been placed into three general categories: rhizosphere biofilms (or root biofilms), epiphytic biofilms (biofilms on plant surfaces) and endophytic/vascular biofilm (biofilms inside plant tissues). An example of a rhizosphere biofilm-producing bacterium is *Pseudomonas fluorescens*. *P. fluorescens* is used as a biocontrol bacterium that forms bacterial biofilm-like aggregates on rice and wheat roots, which leads to increased resistance to root fungal infection (Couillerot et al. 2009). Couillerot et al. (2009) observed that *P. fluorescens* cells expressing fluorescent proteins formed aggregates in the grooves between root epidermal cells. Another *Pseudomonas* bacterium, *Pseudomonas putida*, colonizes corn root surfaces by forming microcolonies (Espinosa-Urgel, Kolter, and Ramos, 2002). In addition, during *Rhizobia*-plant interactions, Fujishige et al. (2006) used beta-glucuronidase (GUS)-labeled *Sinorhizobium meliloti* to show the presence of bacterial aggregates in alfalfa nodules, suggesting that *S. meliloti* forms biofilms in nodules. Additionally, *S. meliloti* may form biofilms on root surfaces and aggregate formation on root hairs may contribute to alfalfa nodulation (Fujishige et al., 2006). Furthermore, a *S. meliloti* strain that produces 57%-60% less exopolysaccharide than wild type *in vitro* also displayed reduced ability to induce nodulation in alfalfa roots (Fujishige et al. 2006). Fujishige et al. (2006) also found that there was no *S. meliloti* mutant colonization in nodules when alfalfa roots

were inoculated with the *S. meliloti* exopolysaccharide mutant, suggesting that ability to produce exopolysaccharide and form aggregates aids in nodulation of plant roots. Therefore, these experiments provide evidence that some bacteria interact with plant hosts via biofilm formation to achieve mutualism (Fujishige et al. 2006).

In addition to colonizing plant roots, some plant-associated bacteria have an epiphytic phase (living on leaf surfaces) before entering the plant intercellular space. When Bacterial colonization of plants starts with landing on plant surfaces via wind or water (e.g., rain splash) unless wounding or other physical damage caused by insect occurs to provide access to the inside of the plant tissue. Bacteria may encounter unpredictable water availability on the surface of plants, therefore forming biofilms may be beneficial to protect bacteria from environmental stresses (Danhorn and Fuqua 2007). For example, *Pseudomonas syringae* pv. *syringae* (*Pss*) colonizes bean leaves epiphytically and causes brown spot disease after entering leaf intercellular spaces (Monier and Lindow 2004). Using epifluorescence microscopy and image analysis, Monier and Lindow (2004) found that *Pss* forms aggregates of bacterial cells on the surface of bean leaves. In addition, they found that larger aggregates were more tolerant of desiccation than solitary cells. Monier and Lindow (2004) stated that epiphytic aggregates of *Pss* grown at lower humidity/ water availability share similar properties with aggregates of *Pss* growing in leaf intercellular spaces and in liquid media *in vitro* which has higher humidity/water availability to bacteria, suggesting

that *Pss* biofilms forming under different conditions may be similar and water availability does not affect biofilm formation. However, they did not look into the composition of *Pss* biofilms, therefore they cannot rule out that *Pss* may form biofilms with different extracellular components under different conditions even though the biofilm-like aggregate formation appears to be similar. Furthermore, *Pss* mutants defective in alginate exopolysaccharide production were more susceptible to hydrogen peroxide treatment *in vitro* (Quiñones, Dulla, and Lindow 2005). Together, this suggests that the ability to form biofilm-like aggregates may contribute to bacterial tolerance of the unfavorable conditions on the leaf surface.

Lastly, endophytic pathogens colonize plant intercellular spaces and cause diseases. For example, *Xylella fastidiosa* is a endophytic pathogen that causes Pierce's disease in grapevines, and variegated chlorosis disease in citrus (Danhorn and Fuqua 2007). Insects act as a natural vector for *X. fastidiosa* when insects feed on xylem sap. *X. fastidiosa* then attaches to the inner walls of xylem vessels by forming aggregates and producing lipopolysaccharides (LPSs) and surface bacterial components such as flagella, pilli and fimbriae (Clifford, Rapicavoli, and Roper 2013; Cava et al. 1989). In addition to *X. fastidiosa*, *Erwinia amylovora* (a virulent pathogen in apple and pear trees) was shown to produce the exopolysaccharides, amylovoran and levan, thought to be important components in *Erwinia* aggregate formation and amylovoran was found to be a pathogenicity factor thought to protect bacterial cells from plant-produced antimicrobials (Koczan et al. 2009). Koczan et al. (2009) examined symptoms

caused by wild-type *E. amylovora* and an amylovoran-biosynthesis mutant in pear fruits. Wild-type bacterial cells were observed on the inner walls of the xylem vessels in leaf cross sections using electron scanning microscopy. Additionally, wild-type *E. amylovora* attached to the inner walls of the xylem vessels forming aggregates embedded in an extracellular matrix as demonstrated using electron scanning microscopy, suggesting that *Erwinia* formed biofilms within the xylem. However, the *E. amylovora* amylovoran-biosynthesis mutant did not cause symptoms in pear fruit and formed no aggregates and no extracellular matrix in apple shoots, suggesting that *E. amylovoran* forms biofilms as part of successful infections of pear (Koczan et al. 2009). Altogether, these studies provide clear evidence that many plant pathogens forms aggregates during infection suggesting biofilm formation is important for plant-microbe interactions. However, there are few studies that examined the signaling events responsible for biofilm formation *P. syringae* bacteria.

Once attached to plant cells, reproduction and aggregate formation of *Pss* are controlled by a quorum-sensing signal called *N-acyl homoserine lactone (AHL)* (Quiñones, Pujol, and Lindow 2004; Quiñones, Dulla, and Lindow 2005). AHL is the quorum sensing signal involved in regulating the production of the exopolysaccharide alginate, as demonstrated by *in vitro* experiments in which the AHL *Pss* mutant produced much less alginate and milder symptoms compared to wildtype *Pss* (Quiñones, Pujol, and Lindow 2004; Quiñones, Dulla, and Lindow 2005). These studies suggest that plant-associated bacterial pathogens may use

quorum sensing to initiate biofilm formation. *Pst* has quorum sensing signaling genes in its genome that are similar to other *Pseudomonas* bacteria (Buell et al. 2003). Additionally, *Pst* produces AHL in KB medium (Chatterjee et al. 2007), however the involvement of quorum sensing signaling to initiate biofilm formation in the *Arabidopsis-Pst* interaction has not been investigated. However, *Pst* colonies and aggregates have been observed in leaf intercellular spaces using fluorescence microscopy and electron microscopy, leading to the idea that *Pst* forms biofilms during infection of plants (Badel et al. 2002; Boureau et al. 2002; Varvaro, Fanigliulo, and Babelegoto 1993; Whalen et al. 1991).

1.3.1 Biofilm matrix components

During infection of *Arabidopsis*, *Pst* is thought to form biofilms to protect the bacterial cells from environmental stress such as host immune responses in leaf intercellular spaces (Wilson et al. 2017). Given that the ability to produce EPS appears to be involved in pathogenicity in some bacteria (e.g. *Pss* and *E. amylovoran*) (Yu et al. 1999; Quiñones, Pujol, and Lindow 2004; Koczan et al. 2009) EPS biosynthesis may be important for successful infection by *Pst*. In terms of biofilm matrix components found in other *Pseudomonas* species, *Pst* contains the genomic loci for synthesis of cellulose, levan, and alginate (Buell et al. 2003). However, only cellulose and alginate were produced by *Pst* during *in vitro* studies (Pérez-mendoza et al. 2019; Fett and Dunn 1989). The EPS levan has not yet been observed in *Pst* biofilm studies *in vitro* or *in vivo*. However, a study identified homologs of levansucrase that may be responsible for levan

biosynthesis (Visnapuu et al. 2011). To date, few studies have been performed to identify the specific components of *Pst* biofilms. Nonetheless, studies of other *Pseudomonas syringae* pathovars and *Pseudomonas* species may provide knowledge to inform studies on *Pst* biofilm formation.

Levan is a beta-branched polyfructan synthesized from sucrose by the extracellular enzyme levansucrase in *Psg* (Osman et al. 1986). In an *in vitro* study, *Psg* was grown in a continuous flow system to encourage the formation of large biofilms because fresh nutrients were constantly supplied and metabolic wastes were constantly removed (Laue et al. 2006). These authors observed that concanavalin A (ConA), a fluorescently labeled lectin, bound to the mannuronic acid subunits of alginate in *P. aeruginosa* biofilms (Strathmann, Wingender, and Flemming 2002). However, ConA did not bind to biofilms produced by wild-type *Psg*, suggesting that alginate is not a major *Psg* biofilm component. However, ConA localized to the spaces between bacterial cells in developing biofilms produced by alginate-deficient levan-producing *Psg*, suggesting that ConA also detects levan in *Psg* biofilms. To confirm that ConA was binding to levan, *Psg* biofilms were treated with an enzyme to digest levan and ConA binding was abolished (Laue et al. 2006). In addition, levan was not detected by Gas Chromatography-Mass Spectrometry (GC-MS) in *Psg* isolated from infected soybean leaves (Osman et al. 1986), suggesting that *Psg* bacteria form biofilms differently under different conditions (*in vivo* vs. *in vitro*). Altogether, this suggests that levan is a component of *Psg* biofilms *in vitro*. Since *Psg* and *Pst* are

pathovars of *P. syringae* and the levansucrase biosynthesis gene has been identified in *Pst* (Visnapuu et al. 2011), this leads to the idea that levan may be a component of *Pst* biofilms.

Cellulose is a polysaccharide composed of beta-(1,4)-linked glucose subunits that is widely found in plant cell walls (Mitra and Loqué 2014) and in *Pst* biofilms grown *in vitro* (Pérez-mendoza et al. 2019). Mitra and Loqué (2014) used calcofluor white (CFW), a fluorescent dye that binds to the beta-(1,4)-glucose linkages of cellulose to demonstrate the presence of cellulose within *Pst* biofilms *in vitro* (Ude et al. 2006) and its absence in cellulose synthase mutant *Pst* biofilms, suggesting that cellulose is a component of *Pst* biofilms (Farias and Olmedilla 2019). However, cellulose synthase mutant *Pst* reached similar *in planta* bacterial levels over 10 days in tomato leaves compared to wild-type *Pst*, suggesting that the ability to produce cellulose is not necessary for bacterial success in tomato (Prada-ramírez et al. 2016). Moreover, *Pst* expression data indicated that *Pst* cellulose synthase was highly expressed during Effector-Triggered Immunity (ETI) triggered by the *Pst* effector, AvrRpt2. In contrast, little cellulose synthase expression was detected when virulent *Pst* successfully caused disease on *Arabidopsis* (Nobori et al. 2018), perhaps because virulent *Pst* suppresses the plant defense, making production of cellulose and biofilms unnecessary for bacterial success *in planta*. These data collectively support the idea that cellulose and biofilms are important for *Pst* to withstand plant defense.

1.3.1.1 Alginate in bacterial biofilms

In addition to levan and cellulose, alginate is the biofilm component that has been identified in *Pseudomonas* biofilms and examined in many studies. Alginate is a copolymer of beta-(1,4)-mannuronic and alpha-(1,4)-guluronic acid (Grasdalen 1983). Using Nuclear Magnetic Resonance (NMR), alginate was detected in liquid *Psg* cultures grown with glucose as the primary carbon source and also in lyophilized water extracts collected from *Psg*-infected soybean leaves, suggesting *Psg* produces alginate *in vitro* and *in vivo* (Osman et al. 1986). In addition, *Pss* mutants that produced little alginate were more susceptible to hydrogen peroxide treatment *in vitro*, suggesting that alginate may contribute to bacterial tolerance of antimicrobials such as hydrogen peroxide (Quiñones, Dulla, and Lindow 2005). Alginate-deficient *Pss* mutants also lost the ability to swarm out of the original inoculation site on King's Broth (KB) plates while wild-type *Pss* was able to swarm outwards, suggesting that alginate may contribute to swarming mobility (Quiñones, Dulla, and Lindow 2005). Most importantly, alginate-deficient *Pss* did not cause any visible lesions, while wild-type *Pss* caused significant damage and lesions in bean pods (drop inoculation with 5×10^7 bacterial cells) (Quiñones, Dulla, and Lindow 2005). These studies suggest that the ability to produce alginate contributes to the pathogenicity of some *Pseudomonas* bacteria. A recent study with *Pst* reported that the alginate-deficient mutant $\Delta algD$ *Pst* caused typical necrotic lesions on tomato leaves just like wild-type *Pst*, but with less chlorosis compared to the wild type (Ishiga et al. 2018). Interestingly, the $\Delta algD$ *Pst* mutant reached the same levels as wild-type

Pst in planta (Ishiga et al. 2018). Similar results were also found in *Arabidopsis* two week-old seedlings grown on plates (Ishiga et al. 2018), supporting the idea that alginate does not have a major role in *Pst* pathogenicity or bacterial success.

1.3.1.2 Alginate Biosynthesis

Alginate biosynthesis has been thoroughly studied in *P. aeruginosa* (Rasamiravaka et al. 2015). In *P. aeruginosa*, alginate biosynthesis genes are contained within a single 12-gene operon (*AlgD*, *Alg8*, *Alg44*, *AlgK*, *AlgE* (*AlgJ*), *AlgG*, *AlgX*, *AlgL*, *AlgI*, *AlgJ* (*AlgV*), *AlgF*, *AlgA*) described by Chitnis and Ohman (1993) and summarized by Hay et al. (2013). *AlgA*, *AlgC* catalyze the conversion of fructose-6-phosphate to guanosine diphospho-D-mannose (GDP-D-mannose) in several steps. The *AlgD* gene encodes a GDP-D-mannose dehydrogenase and *AlgD* catalyzes the oxidation of GDP-D-mannose to GDP-D-mannuronic acid, which is the final step of precursor synthesis for alginate polymerization (Fakhr et al. 1999). The rest of the genes in the operon are believed to form a transmembrane protein complex to catalyze polymerization (*Alg8* and *Alg44*), acetylation (*AlgI*, *AlgJ*, *AlgF*, *AlgX*), epimerization (*AlgG*) and eventually export the final alginate product to the extracellular space via *AlgK* and *AlgE* (Hay et al. 2013). Regulation of the alginate biosynthesis operon appears to involve over a dozen regulators in *P. aeruginosa* (Hay et al. 2013) including the alginate regulatory operon, *AlgU MucAB*. This regulatory operon has been studied in various *Pseudomonas* species and found to play very similar regulatory roles as it does in *P. aeruginosa* (Hay et al 2013). In *Pss*, homologs of *AlgD*, *Alg8*, *Alg44*,

AlgG, *AlgX*, *AlgL*, *AlgF*, and *AlgA* are present in a gene cluster with a similar order as the cluster in *P. aeruginosa* (Peñaloza-Vázquez et al. 1997). In *Pst*, all of the genes required for alginate biosynthesis as well as *AlgU* and *MucAB* have been identified in a complete *Pst* genome sequencing study (Buell et al. 2003). These results suggest that alginate biosynthesis in *P. syringae* may be similar to that in *P. aeruginosa*.

1.3.1.3 AlgD

AlgD is the first gene transcribed in the alginate gene cluster of *Pst*. AlgD catalyzes production of alginate precursors that polymerize into alginate (Fakhr et al. 1999). Therefore, alginate polymers are not synthesized when AlgD is not functional. In previous studies, the *Pst* Δ *algD* mutant caused less chlorosis compared to wild-type *Pst* in *Arabidopsis* and tomato leaves, suggesting that the ability to produce alginate contributes to *Pst* pathogenicity (Ishiga et al. 2018). Keith and his team (2003) observed *Pst* *AlgD* promoter activity only in tomato leaves undergoing ETI which includes the Hypersensitive Response (HR), suggesting that alginate production is not activated until plants undergo the HR and therefore alginate may play a role in *Pst*'s ability to tolerate the HR. It is believed that *AlgD* expression is activated in response to the presence of plant defense molecules, such as ROS that have been shown to play an important role in PTI (Kadota et al. 2014). In *Pst*, activator OxyR is a key transcription factor expressed when bacteria sense plant-produced hydrogen peroxide to activate the expression of hydrogen peroxide-inducible genes to promote oxidative stress

tolerance in *Pst* during PTI (Ishiga and Ichinose 2016). Ishiga and Ichinose (2016) thought that *AlgD* might be activated in responses to plant-produced ROS, therefore they examined the *AlgD* gene expression levels in a $\Delta oxyR$ *Pst* mutant. They found that $\Delta oxyR$ *Pst* were more susceptible to hydrogen peroxide treatment and *AlgD* transcription levels in $\Delta oxyR$ *Pst* mutants were 10-fold less than wild-type *Pst* at 72 hours post inoculation in *Arabidopsis* (Ishiga and Ichinose 2016). Together, these data suggest that *AlgD* expression is activated in response to plant-produced ROS *in planta* and alginate production may be a bacterial response to plant antimicrobial molecules.

1.3.1.4 AlgU

The *AlgU* gene encodes a sigma factor that regulates genes in the alginate biosynthesis operon including *AlgD*. In addition, *algU* mutant *Pst* showed reduced *HrpL* expression *in vitro* and *in vivo* (flood-inoculated 2-week-old *Arabidopsis*), indicating that AlgU contributes to expression of *HrpL* genes (Ishiga et al. 2018). Since HrpL is an alternative RNA polymerase sigma factor that is involved in regulating many T3SS effectors during *Pst* infection (Fouts et al. 2002), this suggests that AlgU is involved in T3SS-related pathogenesis of *Pst* in *Arabidopsis* in addition to regulating alginate production. Moreover, AlgU is thought to be involved in regulating coronatine production to re-open plant stomata as demonstrated in experiments in which the $\Delta algU$ *Pst* mutant failed to reopen stomata after PTI-induced stomatal closure (Ishiga et al. 2018). This phenotype was rescued by dip-inoculating the mutant with coronatine (100ng/ml),

suggesting that AlgU promotes PTI suppression by regulating coronatine production (Ishiga et al. 2018). Together, these studies led to the idea that AlgU contributes to suppression of PTI by regulating coronatine production and HrpL regulated T3SS-dependent pathogenicity.

1.4 Intercellular SA accumulation contributes to ARR as an antibiofilm agent

SA has been mainly studied for its signaling roles during plant immune defenses and *Pst* is known to suppress SA accumulation and SA-mediated signaling pathways (Xin and He 2013). However, *Pst* also displays sensitivity to direct SA treatments *in vitro*, suggesting that SA also has direct effects on *Pst* growth *in planta* (Wilson et al. 2017). Wilson *et al.* (2017) demonstrated that *Pst* biofilm formation was reduced *in vitro* at SA concentrations of 2 to 10 μM , whereas *in vitro* *Pst* growth reduction occurred at much higher SA concentrations (100 to 200 μM). Complete inhibition of growth happens at SA concentrations of 1mM *in vitro*. SA concentrations of 40 to 100 μM were observed in leaf intercellular washing fluids collected from mature plants during ARR, suggesting that intercellular SA accumulation may contribute to bacterial biofilm suppression. To directly observe biofilm-like aggregate formation *in planta* during ARR, young and mature plants were inoculated with GFP-expressing *Pst* and aggregate formation (defined as a group of tightly packed and immobile cells) was monitored along with leaf intercellular SA concentrations (Wilson et al. 2017). A simultaneous reduction in bacterial aggregates and accumulation of intercellular

SA (40 to 100 μ M) was observed along with reduced bacterial growth in mature plants displaying ARR compared to susceptible young plants. These data suggest that SA accumulation in the intercellular space reduced either *Pst* growth, biofilm formation, or both during ARR (Wilson *et al.* 2017). The antibiofilm properties of SA have also been studied in animal pathogens. SA concentrations of 0.01 to 5 mM were observed to reduce *in vitro* bacterial biofilm formation of animal pathogens such as *P. aeruginosa* and *Staphylococcus aureus* (Prithiviraj, Weir, et al. 2005; Yang et al. 2009).

In conclusion, the mechanisms responsible for restriction of pathogen growth in young plants is poorly understood compared to mature ARR-competent plants that accumulate intercellular SA at levels that inhibit *in vitro* *Pst* biofilm formation. In addition, the contribution of biofilm formation to *Pst* pathogenicity remains uncharacterized. Given that other plant immune responses, like PTI are also SA-dependent, the role of intercellular SA accumulation in suppressing *Pst* biofilm formation during PTI was investigated in this thesis, along with examining the role of biofilm formation in *Pst* pathogenicity and success *in planta*.

1.5 Hypotheses and Objectives

Hypothesis 1: The ability to form biofilms contributes to successful infection by *Pst*.

Objectives:

1A. Examine if biofilm-like aggregate formation is correlated with bacterial growth *in planta*.

1B. Investigate if the ability to produce alginate contributes to bacterial success and pathogenicity of *Pst* by examining biofilm formation *in vivo* in wild-type and alginate mutants.

1C. Investigate if AlgU contributes to *Pst* success and pathogenicity by examining aggregate formation *in planta*.

1D. Obtain evidence that *Pst* aggregates are biofilms by staining for common biofilm components.

Hypothesis 2: The PTI defense response includes suppression of biofilm-like aggregate formation by *Pst*.

Objective: Demonstrate that biofilm formation is reduced during the PTI response.

Hypothesis 3: Intercellular SA accumulation during PTI contributes to suppression of *Pst* biofilm formation.

Objective: Investigate intercellular accumulation of SA during PTI.

Chapter 2: Materials and Methods

2.1 *Arabidopsis* plant lines and growth conditions

Col-0, *sid2-2* (Nawrath and Metraux 1999), *fls2* (Kunze et al. 2004) were used in these studies (*sid2-2* and *fls2* are in the Col-0 background). Seeds were surface-sterilized, stratified for 2 days in darkness at 4°C and then plated on Murashige and Skoog medium. Approximately 1 week later, cotyledon-stage seedlings were transplanted to soil (Sunshine Mix #1 or JVK Agro Mix G5)

moistened with 1 g/L of all-purpose 20- 20-20 fertilizer. Growth conditions were $22 \pm 2^\circ\text{C}$, $80\% \pm 10\%$ relative humidity, and 9 h of light (mixed fluorescent and incandescent, 120 to 150 $\mu\text{mol}/\text{m}^2/\text{s}$). Young plants were grown to 3.5 weeks post germination (wpg) before treatment or inoculation.

2.2 Bacterial strains and transformation

All strains of *P. syringae pv. tomato* DC3000 including wild type, wild type carrying pDSK-GFPuv, and mutants were grown in King's Broth (KB) media overnight at room temperature. Mutant *Pst* strains *Pst* $\Delta algD$ (PS392) and *Pst* $\Delta algD\Delta algU\Delta mucAB$ (PS519) (Markel et al. 2016) were transformed with pDSK-GFPuv (Wang et al. 2007) using the triparental mating method. *E. coli* DH5 carrying the GFP plasmid, the helper strain *E. coli* RK600 and recipient strains of *Pst* were grown overnight separately and were centrifuged for 7 min at 1000g. Cell pellets were resuspended with 20 ml of 10 mM MgCl_2 . Centrifugation and cell pellet resuspensions were repeated twice to remove any antibiotic residue from the overnight cultures. Each resuspended cell culture (50 μl each strain) were combined in 1ml of KB media to make the mating mixture. After one hour of incubation at room temperature (22°C), 50 μl of the mating mixture was transferred onto an LB plate with rifampicin and kanamycin to select successful transformed *Pst*. The successful transformation of *Pst* with GFP-expressing plasmid was confirmed by examining colonies under a UV lamp (365nm) for GFP fluorescence.

2.3 PTI resistance assays and *in planta* quantitation of bacterial levels

Overnight cultures of *Pst* were grown in KB media to mid-exponential phase. Cells were collected by centrifugation, and resuspended in 10 mM MgCl₂ to 10⁶ cfu/ml and then inoculated by pressure-infiltration into fully expanded leaves using a needleless syringe. Prior to *Pst* inoculation, PTI was induced by treating plants with flg22 or mock-treated. One day later, the same leaves were inoculated with bacterial inoculum, after which bacteria levels in the leaves were determined. For quantification of *in planta* bacterial levels, three biological replicates of eight leaf disks (4 mm diameter) were collected and shaken at 200 rpm for 1 hour in 10 mM MgCl₂ with 0.1% Silwet L-77. Serial dilutions were plated on KB media with kanamycin (50 µg/ml) and rifampicin (100 µg/ml). Plates were incubated at room temperature for 2 days before colonies were counted. Occasionally, to slow the growth rate of the bacteria down, the plates were incubated at +4°C for two days and then incubated at room temperature for 10-12 hours before being counted.

2.4 Imaging of *Pst* in the intercellular space by fluorescence microscopy during PTI

Plants were infiltrated with 1µM flg22 peptide (PhytoTech Labs #P6622) or mock-treated with sterile water. Twenty-four hours later the same leaves were inoculated with 10⁶ cfu/ml *Pst* pDSK-GFPuv (Wang *et al.* 2007). After 48 hours, leaves were cut at the petiole and sections of the lower epidermis were removed

using invisible tape. Sections without the lower epidermis were isolated using a razor blade and were mounted in water on a glass slide with the epidermis-less surface facing upwards. Slides were imaged immediately using a Nikon Eclipse E800 microscope fitted with a Nikon DS-Fi1 camera head and the DS-U3 control unit using 100× oil immersion lenses and a B-2A filter cube. For comparing the proportion of cell types between flg22-treated and mock-treated plants of different genotypes, tissue preparation and imaging were performed by different individuals so that the scoring was blind. Aggregate size was measured using ImageJ software (US National Institutes of Health).

2.5 Biofilm matrix staining

Plants were inoculated with 10^6 cfu/ml *Pst* pDSK-GFPuv (Wang et al. 2007). After 48 hours, leaves were cut at the petiole and sections of the lower epidermis were removed using invisible tape. Sections without the lower epidermis were isolated using a razor blade and were mounted on a glass slide with the epidermis-less surface facing upwards. Different leaves were used for staining eDNA and extracellular polysaccharides:

Extracellular DNA Detection

DAPI stock solution (2mg of DAPI powder in 1ml of sterile, deionized water) was added (2.5 μ l) to 100ml sterile deionised water to make a DAPI working solution (0.1 μ g/ml). The working DAPI solution was added to cover the entire

sample (15-30 μl per sample) and samples were incubated in the dark for 5 mins. After incubation, the staining solution was removed using a pipette and 50 μl of sterile deionised water was gently pipetted onto the samples to rinse them. This procedure was repeated three times. After removing excess liquid, a cover slip was gently placed on each slide. A UV filter (435-485 nm) was used during fluorescence microscopy using the Zeiss Axioskop epifluorescence microscope.

Extracellular Polysaccharide Detection

Concanavalin A, Tetramethylrhodamine Conjugate (ConA-TRIC, Invitrogen™ by ThermoFisher, Cat #: C860) stock solution (2 $\mu\text{g}/\mu\text{l}$) was diluted to working concentration (0.4 $\mu\text{g}/\mu\text{l}$) with PBS buffer. To stain α -polysaccharides, ConA-TRIC working solution was added to cover the entire sample (15-30 μl per sample) and samples were incubated in the dark for 30 mins. After incubation, the staining solution was removed using a pipette and 50 μl of PBS buffer was gently pipetted onto the samples to rise them once. After ConA-TRIC staining, the Calcofluor White (CFW, Sigma-Aldrich, Cat# 18909-100ML-F) working dye solution was prepared by mixing CFW stock solution with 10% KOH solution in a ratio of 3:2. The CFW working dye solution was pipetted (15-30 μl per sample) to cover the samples to stain β -polysaccharides. Slides were incubated in the dark for 5 mins at 22°C. After incubation, the dye solution was removed, and sterile water was pipetted onto the slide to rinse the samples. The excess liquid was removed, and a cover slip was gently placed on each slide. A Cy5 filter (663-738

nm) was used to observe ConA-TRIC signals, and a UV filter (435-485 nm) was used to observe CFW signals during fluorescence microscopy using the Zeiss Axioskop epifluorescence microscope.

2.6 Intercellular washing fluid (IWF) collection

The technique for infiltration of leaves and collection of IWFs was adapted from Baker *et al.* (2012) and O'Leary *et al.* (2014) – see this reference for a video demonstration of the technique. Three pools of 8-12 leaves were cut at the petiole, weighed and then vacuum-infiltrated with water inside a 60 ml syringe until they appeared completely water-soaked. Leaves were then blotted dry, stacked between parafilm sheets, rolled around a 1 ml pipette tip, secured with a twist-tie, and placed inside the bottom third of a 60 ml syringe fitted to a 1.5 ml centrifuge tube with the petioles facing up. Leaves were then centrifuged using a swinging bucket rotor at 600 x g for 15 minutes at room temperature to collect the IWFs. The IWFs were centrifuged for an additional 5 minutes at 13,000 x g, transferred to fresh tubes, weighed, and stored at -80°C. The remaining pellets (chlorophyll sometimes visible) were resuspended in 1 ml of ethanol and measured spectrophotometrically at 664 and 700 nm to assess contamination of IWFs with cellular contents (Baker *et al.* 2012). In a representative experiment, the chlorophyll levels in IWFs were 0.85 percent of the corresponding leaf tissue, indicating that the IWFs had minimal cellular contamination.

2.7 Biosensor SA quantification

SA was quantified using the ADPWH_lux SA biosensor (Defraia, Schmelz, and Mou 2008) as described previously by Carviel et al. (2014).

2.8 Statistical tests

Statistical significance was determined using a Student's t-test or an analysis of variance (ANOVA), or Kruskal-Wallis test as indicated. For the student's t-test, a two-tailed test for either equal or unequal variance was performed where $p < 0.05$. Single variable ANOVA analysis was performed with $p < 0.05$ and followed up with a Post HOC test, Tukey's HSD. Kruskal-Wallis test was performed with $p < 0.05$ and followed by Dunn's test.

Chapter 3: Investigating biofilm formation by *Pseudomonas syringae* pv. *tomato* and the effect of PAMP-Triggered Immunity on bacterial biofilm formation in *Arabidopsis*

3.1 Preface

In vitro and *in vivo* studies suggest that intercellular SA accumulates and acts as an antibiofilm agent against *Pst* during ARR (Carviel *et al.* 2014, Wilson *et al.* 2017). These studies led us to investigate if *Pst* forms biofilm-like aggregates that contribute to bacterial pathogenicity and success during infection of young susceptible *Arabidopsis*. Additionally, experiments were conducted to determine if the *Arabidopsis* PTI response includes suppression of *Pst* biofilm formation to reduce bacterial multiplication and success.

3.2 Author contributions

Noah Xiao (NX), Angela Fufeng (AF), Garrett Nunn (GN), Abdul Halim (AH) and Natalie Belu (NB) contributed to the experiments. NX and AF performed all bacterial growth and aggregation formation experiments shown in all relevant tables and figures. NX transformed GFP-expressing alginate mutant *Pst* and conducted aggregate size and number analysis on ImageJ and R. Biofilm staining experiments were conceived by RC and AH, optimized by RC and NX, and performed by NX and AH. Intercellular washing fluid were collected by NX with significant contributions from GN and NB. NX performed all SA quantitation assays. Experiments (except biofilm staining) were conceived and developed by

RC, NX and AF. NX will write the first draft of manuscript as the first author and NX and RC will edit the manuscript as corresponding author with help from AF, GN, AH and NB.

3.3 Bacterial aggregate formation is associated with successful infection by *Pst*

There is evidence supporting the idea that some plant pathogens form biofilms during infection and that the ability to form biofilms contributes to bacterial success *in planta* (Dow et al. 2003; Monier and Lindow 2004; Quiñones, Dulla, and Lindow 2005; Laue et al. 2006; Rasamiravaka et al. 2015; Nobori et al. 2018). Wilson et al. (2017) provided compelling evidence that intercellular SA accumulation reduces *Pst* biofilm-like aggregate formation during the ARR response. A number of studies have demonstrated that *P. aeruginosa* forms multicellular aggregate biofilms during infection of human lungs (Kragh et al. 2016; Hoiby, Ciofu, and Bjarnsholt 2010). This led to the idea that *Pst* may form biofilm-like aggregates during infection of *Arabidopsis* and that the ability to form biofilm-like aggregates may be associated with *Pst* success and pathogenicity. *Pst* success was determined by measuring *in planta* bacterial levels and bacterial aggregates were observed using a GFP-expressing *Pst* strain to monitor biofilm-like aggregate formation. Leaves were infiltrated with a 1 μ M flg22 peptide solution to induce the PTI response or mock-treated with water to examine the susceptible interaction in which *Pst* is successful. One day later, these same leaves were inoculated with virulent GFP-expressing *Pst* and bacterial levels in

susceptible (mock-treated) and PTI-responding (flg22-treated) leaves were determined 3 days later. At 48 hours post inoculation (hpi), bacterial cell types were also monitored via microscopic examination of GFP-expressing *Pst* in leaf intercellular spaces using epifluorescence microscopy. Bacterial cells were classified as aggregates (biofilm-like), defined as immobile and tightly grouped cells, or planktonic (individual free-swimming cells). Each microscopic field was viewed and classified as containing no bacteria, planktonic bacteria, bacterial aggregates, or both planktonic bacteria and bacterial aggregates, examples can be seen in Figure 1. In these fluorescence microscope images, GFP-expressing *Pst* cell aggregates and planktonic cells with green signals were observed among plant cells with chloroplasts providing auto-fluorescent red signals in leaf intercellular spaces (Figure 1).

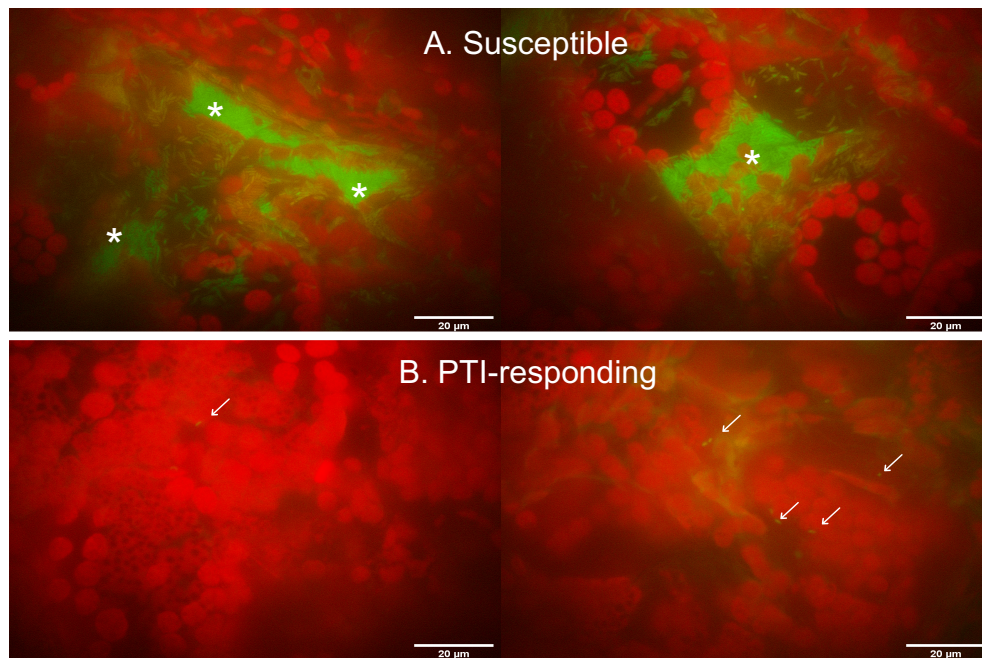


Figure 1. Visualization of GFP-expressing *Pst* in susceptible and PTI-responding leaves. Leaves and bacteria were viewed at 1000X magnification under epifluorescence in A) susceptible mock-treated plants and B) PTI-responding plants. Arrows mark examples of planktonic bacteria, asterisks mark examples of aggregated bacteria.

Overall, *in planta Pst* levels were reduced in flg22-treated plants compared to susceptible mock-treated plants, from 6 to 100-fold in 8 replicate experiments, indicating that the strength of the PTI response varies between experiments (Table 1). In susceptible mock-treated Col-0 leaves, 20 to 80% of the fields of view (FOV) contained bacterial aggregates, while few fields of view were observed to have bacterial aggregates in PTI-responding leaves (Table 2). In 4 of 8 experiments, 3 to 25% of the fields of view contained aggregates in PTI-responding leaves, providing further support that the strength of the PTI response varies between experiments. However, aggregates in PTI-responding leaves were smaller in size than aggregates found in susceptible plants (Fufeng 2019), suggesting that the PTI response results in a reduction in aggregate size, in addition to reducing the number of aggregates that form. Taken together, these data indicate that *Pst* success during infection (high bacterial levels) is associated with the formation of aggregates, and the PTI response may result in suppression of bacterial aggregate formation.

Table 1. PTI response varies across experiments

Genotype	PTI Response in Eight Experiments ¹							
	1	2	3	4	5	6	7	8
Col-0	32	22	100	52	68	9	16	8
<i>fls2</i>	nd ²	nd	nd	nd	nd	nd	nd	nd
<i>sid2-2</i>	nd	7	16	7	5	nd	5	7

¹ Leaves were infiltrated with water (mock-treated) or 1 μ M flg22 (flg22-treated), 24 hours later, the same leaves were inoculated with virulent GFP-expressing *Pst*. *In planta* bacterial levels were determined at 72 hpi. The PTI response was calculated as the statistically significant fold difference in *Pst* levels in leaves that were mock-treated versus flg22-treated. See Table A1 in Appendix A for *Pst* levels. Two-way ANOVA (Tukey's HSD).

² nd = no difference in *Pst* levels between flg22-treated and mock-treated leaves.

Table 2. Percent FOV with *Pst* aggregates in flg22- and mock-treated leaves.

Genotype	Treatment ¹	% FOV with <i>Pst</i> aggregates in leaves ²							
		Experiment ³							
		1	2	3	4	5	6	7	8
Col-0	Mock	75	80	40	60	40	40	20	55
	flg22	0	25	0	0	5	3	0	10
<i>sid2-2</i>	Mock	90	90	90	60	70	60	20	50
	flg22	25	40	50	20	45	20	20	5
<i>fls2</i>	Mock	90	90	70	75	50	70	30	40
	flg22	75	90	30	80	90	80	30	45

¹ Leaves of Col-0, *sid2-2*, and *fls2* were treated with 1 μ M flg22 (flg22-treated) or mock-treated with water. 24 hours later, the same leaves were inoculated with virulent GFP-expressing *Pst*.

² FOV with *Pst* aggregates was determined by categorizing each microscopic field of view as with or without aggregates and calculating the percentage of FOV with aggregates.

³ Table 1 and Table 2 display complementary data for the same 8 experiments.

3.4 The PTI response is associated with reduced bacterial aggregate formation

To investigate if *Pst* aggregate formation is suppressed by the plant PTI response, the effect of PTI on aggregate formation was examined in PTI-competent and incompetent plants. *Pst* levels (Table 1) and aggregate formation (Table 2) were compared in PTI-responding and susceptible wild-type Col-0, *fls2* (PTI flg22 receptor mutant) and *sid2-2* (SA biosynthesis mutant). Col-0 plants treated with flg22 displayed various levels of PTI (8 to 100-fold reduction in *Pst* levels compared to mock-treated Col-0). However, bacterial levels in flg22-treated and mock-treated *fls2* were similarly high as was expected in this flg22 receptor mutant which acts as a negative control for the PTI response in this experiment (Table 1). In 6 of 8 experiments (experiments 2,3,4,5,7,8), 5- to 16-fold reductions in bacterial levels were observed in flg22-treated *sid2-2* plants as

compared to mock-treated *sid2-2* plants, indicating a modest or partial PTI response in *sid2-2* (Table 1). Given that *sid2-2* plants produce little SA, these results suggest the PTI response is predominately, but not exclusively an SA-dependent response.

The effect of the SA-dependent PTI response on *Pst* aggregate formation was also examined in these 8 replicate experiments. In 4 of 8 experiments, none of the fields of view from PTI-responding flg22-treated Col-0 leaves contained *Pst* aggregates (Table 2). In four other experiments (experiments 2,5,3,8), 3 to 25 percent of fields of view contained aggregates in PTI-responding flg22-treated Col-0 leaves, whereas 40 to 80 percent of fields of view contained aggregates in mock-treated, susceptible Col-0 plants. In 7 out of 8 experiments, aggregates were observed in flg22-treated *sid2-2* leaves in 5 to 50% of the fields of view compared to 20 to 90% of the fields of view in mock-treated *sid2-2* plants, indicating a modest or partial suppression of aggregate formation in *sid2-2* that also displayed a modest or partial PTI response. This suggests that biofilm-like aggregate suppression during PTI is predominately SA-dependent. In addition, the percentage of fields of view with aggregates was similar (30 to 90%) in both mock-treated and flg22-treated *fls2* plants among all eight replicate experiments. These *fls2* plants served as a negative control group to show that the reduction of bacterial growth and biofilm-like aggregate formation is due to PTI resulting from flg22-FLS2 interaction. Together, these data provide compelling evidence that the

PTI response results in suppression of bacterial aggregate formation in a predominately SA-dependent manner.

3.5 Visualization of the *Pst* extracellular matrix

Bacterial biofilms are thought to consist of communities of surface-adherent aggregated cells embedded in a self-secreted matrix of EPS (Flemming and Wingender 2010). The EPS matrix of bacterial biofilms is thought to contain bacterial proteins, lipids and eDNA (Mann and Wozniak 2012). To obtain evidence that *Pst* aggregates (Figure 1, Table 2) are biofilms, extracellular matrix components were examined *in planta* using various stains and fluorescence microscopy. The lower epidermal layers of leaves inoculated with GFP-expressing *Pst* were peeled to expose leaf cells and intercellular spaces, then incubated in DAPI staining solution. GFP-expressing *Pst* aggregates were observed using a GFP filter (510nm) and extracellular DNA (eDNA) was observed using a UV filter (435-485 nm) to detect blue DAPI signals. DAPI signals were observed to surround and overlap with *Pst*-GFP aggregates in the merged images in Figure 2A. Since calcofluor white emits signals with a similar wavelength as DAPI, other leaves were peeled and stained with ConA-TRITC and calcofluor white for α - and β -polysaccharides respectively. In addition to GFP-expressing *Pst* aggregates, extracellular α - and β -polysaccharides were detected as red signals (Cy5 filter, 663-738 nm) and blue signals (UV filter, 435 - 485 nm), respectively (Figure 2B). These signals overlapped and surrounded GFP-expressing *Pst* aggregates in the merged images in Figure 2B, suggesting

that GFP-expressing *Pst* were embedded in a matrix of polysaccharides and eDNA and providing compelling evidence that *Pst* bacteria form biofilms *in planta*.

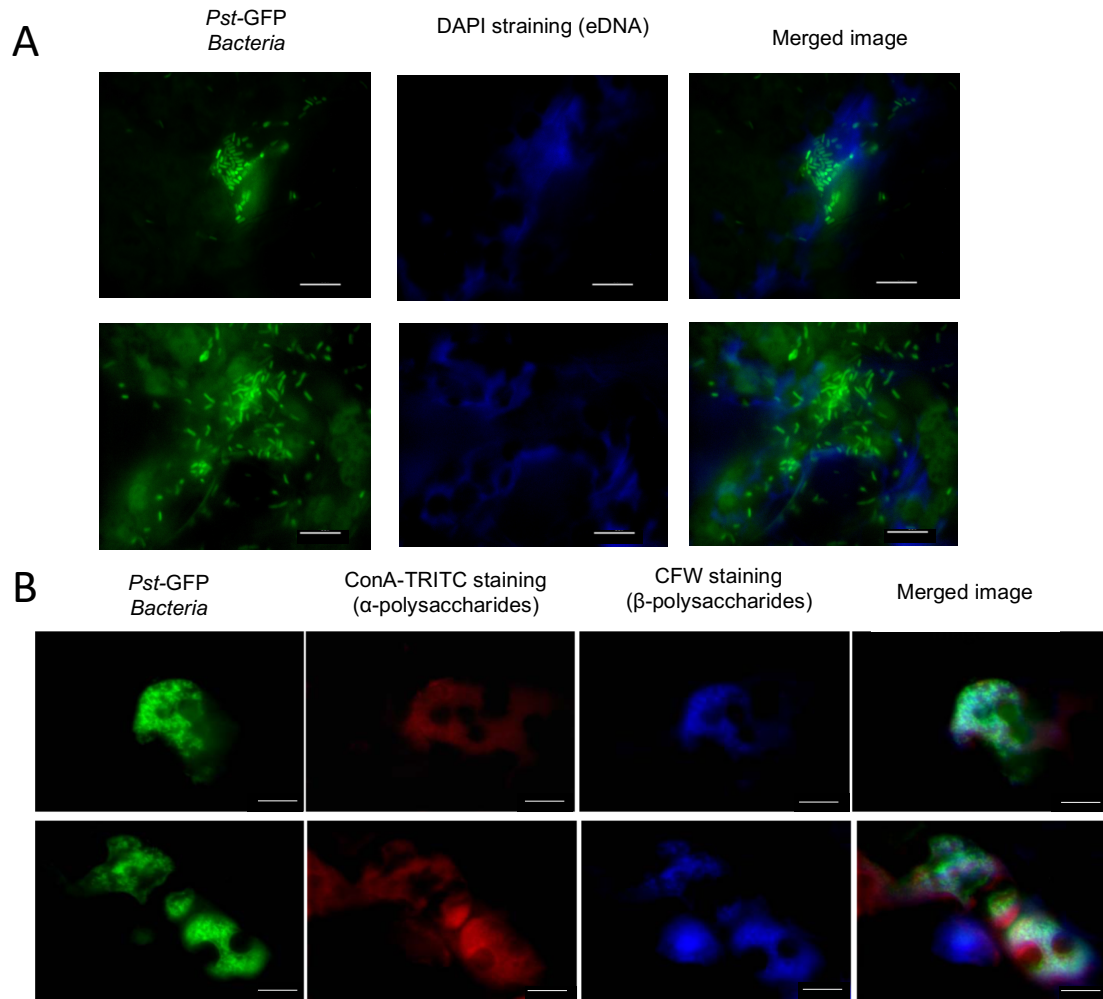


Figure 2. Visualization of the *Pst* extracellular matrix. The epidermis was peeled from leaves inoculated with *Pst*-GFP at 48 hpi, then A) stained with DAPI to visualize extracellular DNA (UV filter, 435-485 nm) or B) calcofluor white (CFW) to visualize β -polysaccharides (UV filter, 435-485 nm) and ConA-TRITC to visualize α -polysaccharides (Cy5 filter, 663-738 nm) using a fluorescence microscope. Scale bar equals 20 μ m. First roll and second roll in A and B are sets of images taken from different leaves. This experiment was repeated once with similar results.

3.6 The ability to produce alginate is not required for *Pst* success *in planta* but contributes to *Pst* aggregate formation

Many studies indicate that alginate is an important component of the extracellular matrix of *P. aeruginosa* biofilms (Rasamiravaka et al. 2015) and *Pst* encodes alginate biosynthesis genes (Buell et al. 2003). Therefore, alginate may be a component of *Pst* biofilms. To examine the contribution of alginate to *Pst* aggregate formation and success, bacterial levels and aggregate formation were monitored in GFP-expressing wild-type *Pst* and *Pst* Δ *algD*, an alginate biosynthesis mutant (Markel et al. 2016), during infection of *Arabidopsis*. If alginate is a major contributor to *Pst* success and biofilm formation, the Δ *algD* mutant will be less successful than wild-type *Pst* in terms of *in planta* bacterial multiplication and aggregate formation. However, both Col-0 and *sid2-2* plants inoculated with wild-type *Pst* and *Pst* Δ *algD* supported similar bacterial levels suggesting that bacterial success was not affected by the absence of alginate biosynthesis (Figure 3A). In Col-0 leaves inoculated with *Pst* Δ *algD*, 55% of the fields of view contained aggregates compared to 78% of fields of view in leaves inoculated with wild-type *Pst*. In Col-0 plants inoculated with *Pst* Δ *algD*, 40% of fields of view contained planktonic bacteria and 5% of the fields of view had no visible bacteria, whereas only 23% of wild-type *Pst*-containing fields of view contained planktonic bacteria suggesting that the ability to produce alginate contributes to *Pst* aggregate formation (Figure 3B). In *sid2-2* SA-deficient leaves, 48% of the fields of view contained both *Pst* Δ *algD* aggregates and planktonic

cells, while 33% of the fields of view contained *Pst* Δ *algD* planktonic bacteria and 20% of the fields of view had no cells. However, in wild-type *Pst*-inoculated *sid2-2* leaves many more fields of view contained aggregates (96%), providing evidence the ability to produce alginate contributes to *Pst* aggregate formation (Figure 3B). Despite an inability to produce alginate, *Pst* Δ *algD* was able to form aggregates, although at a reduced capacity (Figure 3B), suggesting that alginate is a component of *Pst* biofilm-like aggregates.

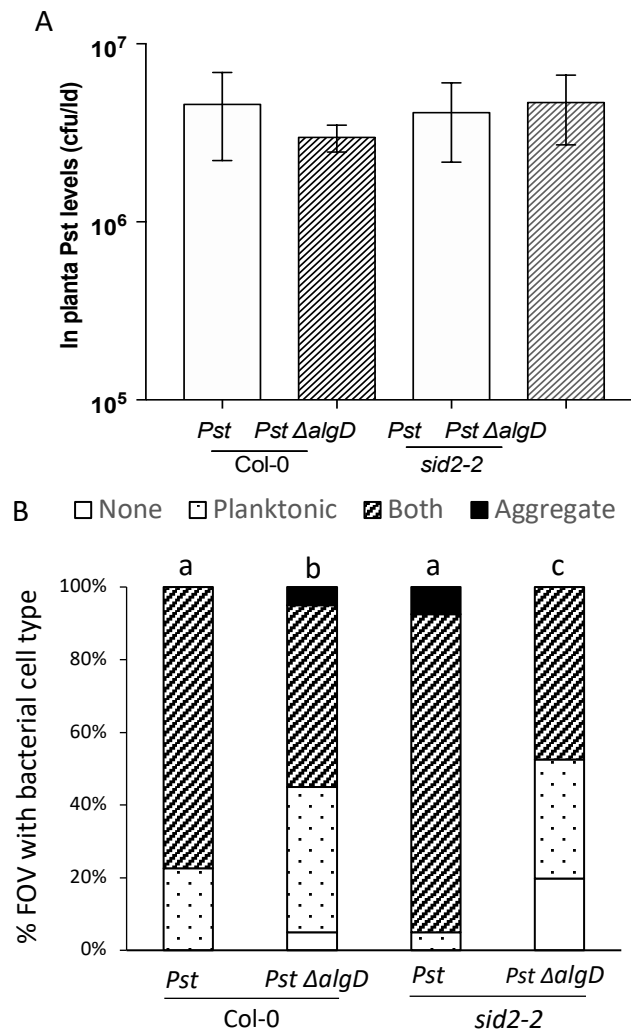


Figure 3. Growth and aggregate formation of *Pst* and *Pst ΔalgD* in Col-0 and *sid2-2*. Leaves were inoculated with GFP-expressing wild-type virulent *Pst* or GFP-expressing alginate biosynthesis mutant *Pst ΔalgD*. A) *In planta* bacterial quantitation of wild-type *Pst*-inoculated and *algD*-inoculated Col-0 and *sid2-2* at 48 hpi. Two-way ANOVA (Tukey's HSD) B) Aggregate formation was monitored by categorizing each microscopic field of view (40 FOV per treatment) as containing no bacteria, only planktonic bacteria, only bacterial aggregates, or both planktonic and bacterial aggregates at 48 hpi. Kruskal-Wallis test. This experiment was repeated 2 additional times with similar results

3.7 Effect of plant-produced SA on *Pst* and *Pst* $\Delta algD$ aggregate formation and size

During the experiment presented in Figure 3, variability in aggregate size was observed among the genotypes and in the presence or absence of SA, hinting that these differences might be informative for understanding the importance of alginate and the effect of plant-produced SA on aggregate formation. Therefore, quantitative aggregate size data was obtained by determining the area of aggregates present in 20 fields of view using ImageJ. The aggregates were categorized as tiny (<100 μm^2), small (100-199 μm^2), medium (200-299 μm^2) or large (>300 μm^2). Examples of aggregate sizes are shown in Figure 4B. Wild type *Pst* formed 30 large aggregates (32 total aggregates) in Col-0 plants, whereas *Pst* $\Delta algD$ formed only 6 large aggregates, 6 medium, 2 small and 4 tiny aggregates (18 in total) (Figure 4A) indicating that in the absence of alginate, *Pst* aggregate numbers and size were reduced. In SA-deficient *sid2-2* leaves *Pst* $\Delta algD$ formed many large aggregates (21 of 24) similar to wild-type *Pst*. These data suggest that alginate may be an important component that allows *Pst* aggregates to withstand the effects of plant-produced SA.

During this analysis it was observed that some fields of view contained many small aggregates, while others contained one very large aggregate that filled most of the field of view and this was not shown in Figure 4A. To provide more information about the differences in aggregate sizes and numbers among the bacterial strains and plant genotypes, the number of aggregates per field of view

was plotted against the size of each aggregate and each data point represents one aggregate (Figure 4C). Local regression lines with 95% confidence intervals were generated using R (scale package) to visualize the correlation between the number of aggregates per field of view and aggregate size. In Figure 4C, the *Pst* $\Delta algD$ in Col-0 regression line is below the regression line for *Pst* with a small overlap of the 95% confident intervals. This statistically supports the observation that *Pst* and *Pst* $\Delta algD$ formed 2, 3 or 4 smaller aggregates (<300 μm^2) per field of view, while *Pst* also formed 1,2,3 or 4 large aggregates (>300 μm^2) per field of view. Thus, the data from Figures 4A and C support the idea that alginate is an important component of *Pst* biofilm-like aggregates. The regression lines for *Pst* and *Pst* $\Delta algD$ in *sid2-2* were closely aligned and the 95% confident intervals were overlapping throughout the regression lines, suggesting that *Pst* $\Delta algD$ and *Pst* formed similar sizes and numbers of aggregates and therefore *Pst* $\Delta algD$ was similarly successful as *Pst* in SA-deficient plants (Figure 4C).

This analysis also sheds light on why the number of *Pst* aggregates was lower in *sid2-2* (20) versus wild-type Col-0 (32). This was unexpected since *Pst* is known to suppress SA-mediated plant defense which contributes to its ability to grow to high levels in wild-type Col-0 (Yuan and He 1996). In looking at Figure 4C, *Pst* formed one very large aggregate in 16 fields of view out of 20 in *sid2-2* leaves, whereas *Pst* formed one very large aggregate in 7 fields of view out of 20 in Col-0 leaves. This may account for the low *Pst* aggregate numbers in *sid2-2* and suggest that *Pst* was as successful or more successful in *sid2-2* compared

to Col-0. Although *Pst* is known to suppress SA-mediated plant defense (Yuan and He 1996), it produced larger aggregates in *sid2-2*, suggesting that *Pst* still benefits from growing in a plant with little SA.

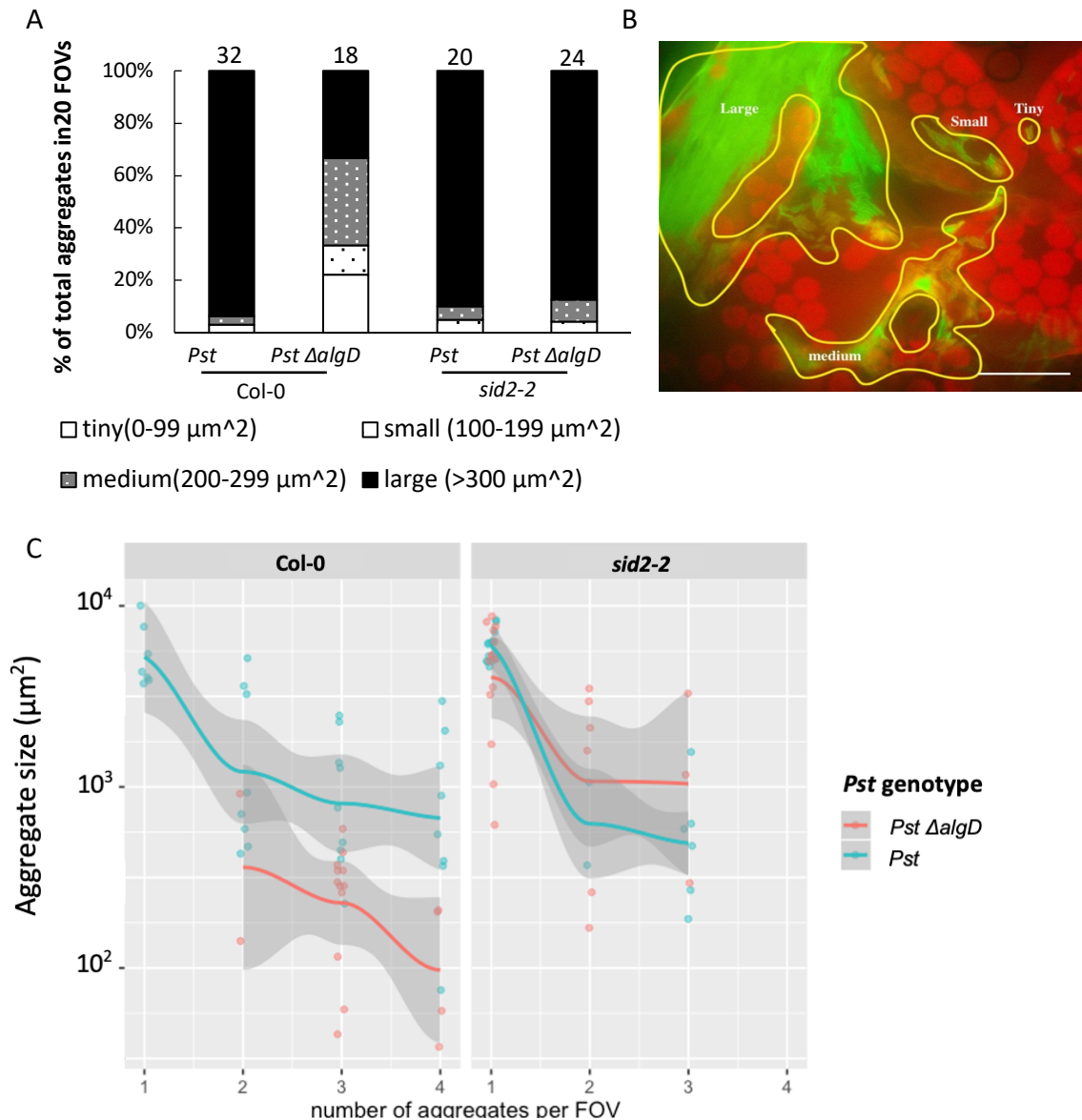


Figure 4. Quantification of aggregate size and number in *Pst* & *Pst ΔalgD* in wild-type Col-0 and *sid2-2*. A) ImageJ was used to calculate the area of each aggregate present in each of 40 fields of view at 48 hpi. The percent of aggregates in each size category was calculated relative to the total number of aggregates. The total number of aggregates in 40 fields of view is indicated above each column. B) example of large, medium, small and tiny aggregates of *Pst ΔalgD* in leaf intercellular spaces at 48hpi. C) Aggregate size in log scale is plotted against the number of aggregates per FOV. Local regression analysis with 95% confident intervals was applied for each bacterial strain in Col-0 and *sid2-2* plants. This experiment was repeated 2 times with similar results.

3.8 Bacterial pathogenicity is associated with the ability to form aggregates

The *Pst* $\Delta algD$ mutant grew as well as *Pst*, probably because it possesses an intact T3SS to deliver plant defense-suppressing effectors into plant cells, therefore the ability to form aggregates was examined in a *Pst* mutant with a reduced ability to proliferate in the intercellular space of tomato plants (Markel et al. 2016). The *Pst* $\Delta algD \Delta algU \Delta mucAB$ produces little alginate, like *Pst* $\Delta algD$, and is also impaired in T3SS regulation and the ability to suppress plant defense responses (Markel et al. 2016). Therefore, this mutant's inability to suppress plant defense should make it possible to observe the effect of the alginate mutation on *Pst*'s ability to infect *Arabidopsis* and to determine if the ability to form aggregates is associated with bacterial success/pathogenicity. A GFP-expressing *Pst* $\Delta algD \Delta algU \Delta mucAB$ strain was created as described in the method section and was compared to wild-type *Pst* in terms of growth and aggregate formation in leaves. Col-0 plants inoculated with *Pst* $\Delta algD \Delta algU \Delta mucAB$ supported 15-fold lower bacterial levels than plants inoculated with wild-type *Pst*, indicating that *Pst* $\Delta algD \Delta algU \Delta mucAB$ was less successful or, in other words, displayed reduced pathogenicity (Figure 5A). In terms of the mutant's ability to form aggregates in wild-type Col-0 leaves, only 13% of the fields of view contained aggregated cells, while wild-type *Pst* aggregates were observed in 93% of the fields of view (Figure 5B). Therefore, *Pst* $\Delta algD \Delta algU \Delta mucAB$ formed far fewer aggregates and grew poorly compared to wild-type *Pst*, suggesting that the plant defense response

was highly effective in suppressing both *Pst* $\Delta algD$ $\Delta algU$ $\Delta mucAB$ growth and aggregate formation.

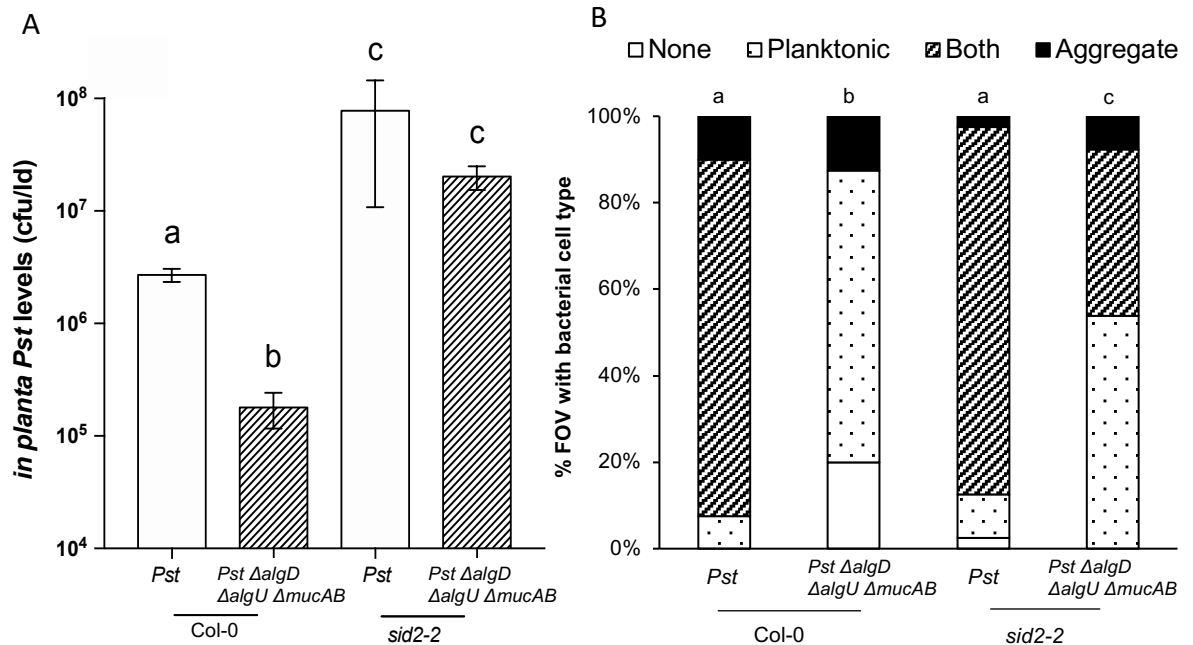


Figure 5. Growth and aggregate formation of *Pst* & *Pst* $\Delta algD$ $\Delta algU$ $\Delta mucAB$ in wild-type Col-0 and *sid2-2*. Leaves were inoculated with GFP-expressing wild-type virulent *Pst* or GFP-expressing alginate biosynthesis mutant *Pst* *algD*. A) *In planta* bacterial quantitation of both strains in Col-0 and *sid2-2* (SA biosynthesis mutant) at 48 hpi. Two-way ANOVA (Tukey's HSD) B) Aggregate formation was monitored by categorizing each microscopic field of view (40 FOV per treatment) as containing no bacteria, only planktonic bacteria, only bacterial aggregates, or both planktonic and bacterial aggregates at 48 hpi. Kruskal-Wallis test. This experiment was repeated 2 times with similar results.

3.9 Effect of plant-produced SA on *Pst* $\Delta algD$ $\Delta algU$ $\Delta mucAB$ aggregate formation and size

SA is an important signaling component in plant defense pathways (Palmer, Shang, and Fu 2017), therefore the effect of SA-mediated defense on *Pst* $\Delta algD$ $\Delta algU$ $\Delta mucAB$ was examined by comparing its growth and aggregate formation in SA-deficient *sid2-2* plants. *Pst* $\Delta algD$ $\Delta algU$ $\Delta mucAB$ grew to higher levels in *sid2-2* compared to Col-0 and reached similar bacterial levels as wild type *Pst* in *sid2-2* plants suggesting plant-produced SA is involved in suppressing *Pst* $\Delta algD$

ΔalgU ΔmucAB growth. Additionally, SA-mediated defense in Col-0 was more effective at reducing *Pst ΔalgD ΔalgU ΔmucAB* levels compared to wild type *Pst* (Figure 5A). A study by Wilson et al. (2017) provided compelling evidence that plant-produced intercellular SA acts as an antibiofilm agent during the ARR response (Wilson et al. 2017). We hypothesize that intercellular SA may also act as an antibiofilm agent during PTI. Therefore, the effect of plant-produced intercellular SA on *Pst ΔalgD ΔalgU ΔmucAB* biofilm-like aggregate formation was investigated. In *sid2-2* plants, 46% of the fields of view contained bacterial aggregates (8% aggregate only, 38% aggregates and planktonic cells) in leaves inoculated with *Pst ΔalgD ΔalgU ΔmucAB* (Figure 5B). However, only 13% of the fields of view contained aggregates when the mutant was growing in Col-0 leaves, suggesting that plant-produced intercellular SA is involved in reducing *Pst* aggregate formation. In addition, it was observed that *Pst ΔalgD ΔalgU ΔmucAB* aggregates were much smaller than aggregates formed by wild type *Pst*. To further examine this observation, the size of each aggregate was measured and the number of aggregates in each field of view was determined. *Pst ΔalgD ΔalgU ΔmucAB* formed almost double the number of aggregates (32 vs 17) along with 80% more medium and large aggregates in *sid2-2* versus Col-0 leaves (Figure 6A). When *Pst ΔalgD ΔalgU ΔmucAB* aggregate number per field of view was plotted against *Pst ΔalgD ΔalgU ΔmucAB* aggregate size, variation in aggregate sizes was observed in both Col-0 and *sid2-2* leaves, and aggregates were smaller when many aggregates were present in the same field of view (Figure

6B). However, in Col-0 leaves inoculated with *Pst*, 17 fields of view contained one very large aggregate (ranged from 725 to 8270 μm^2) and many fields of view contained 2,3,4,5,6 or 7 aggregates, and 50% of these aggregates (39 out of 78 aggregates) were larger in size (253 to 8880 μm^2) than all *Pst* ΔalgD ΔalgU ΔmucAB aggregates (<242 μm^2) in Col-0 leaves (Figure 6B). Although, one field of view contained 7 *Pst* ΔalgD ΔalgU ΔmucAB aggregates in Col-0 leaves, these aggregates included only 1 small (156 μm^2) and 6 tiny (1-99 μm^2) aggregates (Figure 6B). As a result, the local regression analysis calculated different regression lines for wild-type *Pst* and *Pst* ΔalgD ΔalgU ΔmucAB in Col-0, where wild type formed many large aggregates and *Pst* ΔalgD ΔalgU ΔmucAB formed only a few small aggregates (Figure 6B). These results suggest that successful *in planta* bacterial growth is associated with the ability of *Pst* to form large biofilm-like aggregates.

This analysis provides evidence for why the number of aggregates was lower for *Pst* in *sid2-2* (56) versus wild-type Col-0 (95). In looking at Figure 6B, *Pst* formed one very large aggregate in 25 fields of view out of 40 in *sid2-2* leaves, whereas *Pst* formed one very large aggregate in 16 fields of view out of 40 in Col-0 leaves. This may account for the low *Pst* aggregate numbers in *sid2-2* and suggest that *Pst* was as successful or more successful in *sid2-2* compared to Col-0. This provides further support to the idea that although *Pst* suppresses SA-mediated plant defense (Yuan and He 1996), it still benefits from growing in a plant with little SA. In SA-deficient *sid2-2*, *Pst* ΔalgD ΔalgU ΔmucAB formed more

large aggregates ($> 300 \mu\text{m}^2$) compared to Col-0 (22 vs 0) and these large aggregates were similar in size to wild-type *Pst* aggregates in *sid2-2*, suggesting plant-produced SA affects the size and number of biofilm-like aggregates that form *in planta* (Figure 6B). Similar to the results displayed in Figure 4B, the local regression analysis calculated similar regression lines for wild-type *Pst* and *Pst* $\Delta\text{algD } \Delta\text{algU } \Delta\text{mucAB}$ in SA-deficient *sid2-2* leaves, suggesting that in SA-deficient plants, *Pst* and *Pst* $\Delta\text{algD } \Delta\text{algU } \Delta\text{mucAB}$ were similarly successful in terms of growth and aggregate formation. These data provide evidence that plant-produced SA is involved in reducing *Pst* aggregate size and numbers during infection.

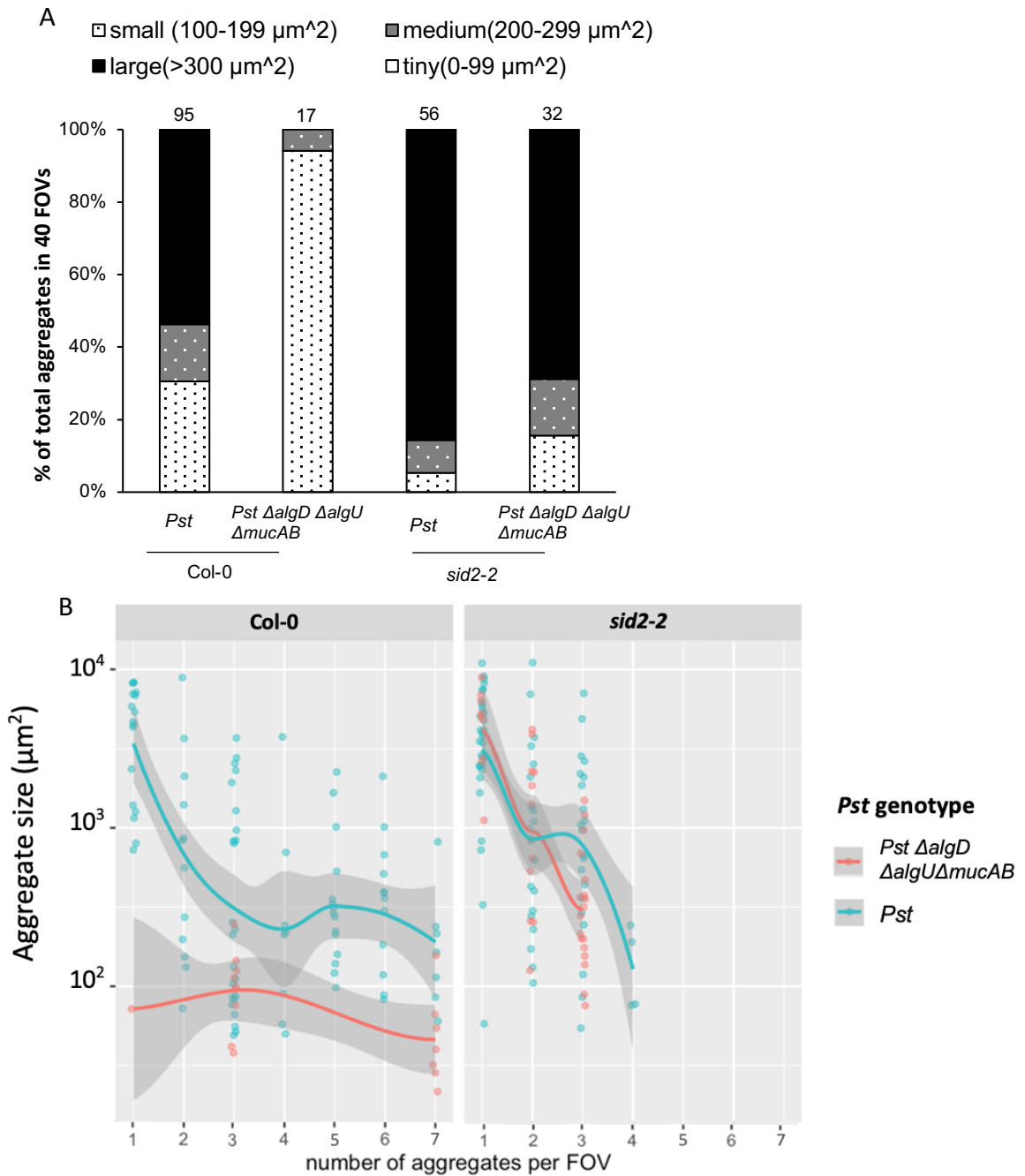


Figure 6. Quantification of aggregate size and number in *Pst* & *Pst* $\Delta algD \Delta algU \Delta mucAB$ in wild-type Col-0 and *sid2-2*. A) ImageJ was used to calculate the area of each aggregates present in 40 fields of view at 48 hpi. The percent of aggregates in each size category was calculated relative to the total number of aggregates. The total number of aggregates in 40 fields of view is indicated above each column. B) Aggregate size is plotted against the number of aggregates per FOV. Local regression analysis with 95% confidence intervals was performed for each bacterial strain grown in Col-0 and *sid2-2* plants. This experiment was repeated 2 times with similar results.

3.10 Early SA accumulation contributes to suppression of bacterial biofilm formation

Given that plant-produced SA is involved in suppressing aggregate formation during *Pst* infection of *Arabidopsis* (Figures 4,5), it is possible that SA acts as an antimicrobial and antibiofilm agent in leaf intercellular spaces during PTI, like it is thought to do during ARR (Wilson et al. 2017). If intercellular SA accumulation contributes to PTI, intercellular SA will be observed in PTI-competent Col-0, but not in the flg22 receptor mutant *fls2*, which is PTI-incompetent. Moreover, *Pst* aggregate numbers should be negatively affected in wild-type Col-0 undergoing the PTI response. As described above, both aggregate numbers and SA levels were determined (SA biosensor assay, see Methods) by collecting intercellular washing fluids (IWFs) from Col-0 and *fls2* leaves that were mock-treated (water) or flg22-treated (induced for PTI) followed by *Pst* inoculation (Figure 7).

Pst levels were monitored in Col-0 leaves to ensure that during this experiment, flg22 treatments induced the PTI response compared to mock-treated Col-0 and to confirm that the *fls2* PTI-defective mutant was PTI-incompetent. Flg22-treated Col-0 supported 20-fold fewer bacteria compared to mock-treated plants, therefore a strong PTI response was observed, while high bacterial levels ($\sim 2 \times 10^6$ cfu/ml) were observed in the PTI-defective mutant *fls2* with and without flg22 treatment, confirming that PTI was not induced (Figure 7A). IWFs from mock-treated plants (Col-0 and *fls2*) contained little intercellular SA at 6, 12, and 24 hours post treatment (< 50 ng/ml). In addition, low levels of SA

were detected (< 550ng/ml) in IWFs collected at 6 and 24 hpi in mock-treated plants (Col-0 and *fls2*). Little SA was detected at 12 hpi with *Pst* in IWFs collected from mock-treated Col-0 and *fls2*. This is consistent with previous work in which young, susceptible Col-0 accumulated little intercellular SA in response to *Pst* (Carviel et al. 2014; Wilson et al. 2017). Moreover, mock-treated plants (Col-0 and *fls2*) that accumulated little SA in leaf intercellular spaces (Figure 7B) were susceptible to *Pst* as indicated by high *in planta* bacterial levels (Figure 7A) and large *Pst* aggregates were observed in mock-treated Col-0 and *fls2* leaves (for all experiments in Table 2). Unlike mock-treated plants, IWFs from flg22-treated PTI-responding Col-0 leaves contained high levels of SA at 6 hours post treatment (hpt) and hpi (1000 – 2050ng/ml) and little biofilm-like aggregate formation was observed in leaf intercellular spaces at 48hpi suggesting that early SA accumulation inhibits the formation of *Pst* biofilm-like aggregate formation (Figure 7B). In contrast, IWFs from flg22-treated *fls2* accumulated little SA (<50ng/ml), similar to mock-treated controls, indicating that intercellular SA accumulation observed in flg22-treated PTI-responding Col-0 is part of the PTI response induced in response to the FLS2-flg22 interaction (Figure 7B). In addition, IWFs from flg22-treated Col-0 plants accumulated moderate levels of intercellular SA at 12 hpi (650ng/ml), whereas little SA was detected in IWFs (<50ng/ml) in other treatment groups. These data suggest that flg22-treated PTI-responding plants rapidly accumulated SA in leaf intercellular spaces to suppress *Pst* biofilm formation. In the absence of flg22-induced PTI, *Pst* successfully suppressed plant

PTI responses including SA accumulation in leaf intercellular spaces (Figure 7B). These results provide evidence that intercellular SA accumulation contributes to the *Arabidopsis* PTI response by suppressing *Pst* biofilm-like aggregate formation and therefore *Pst* bacterial success.

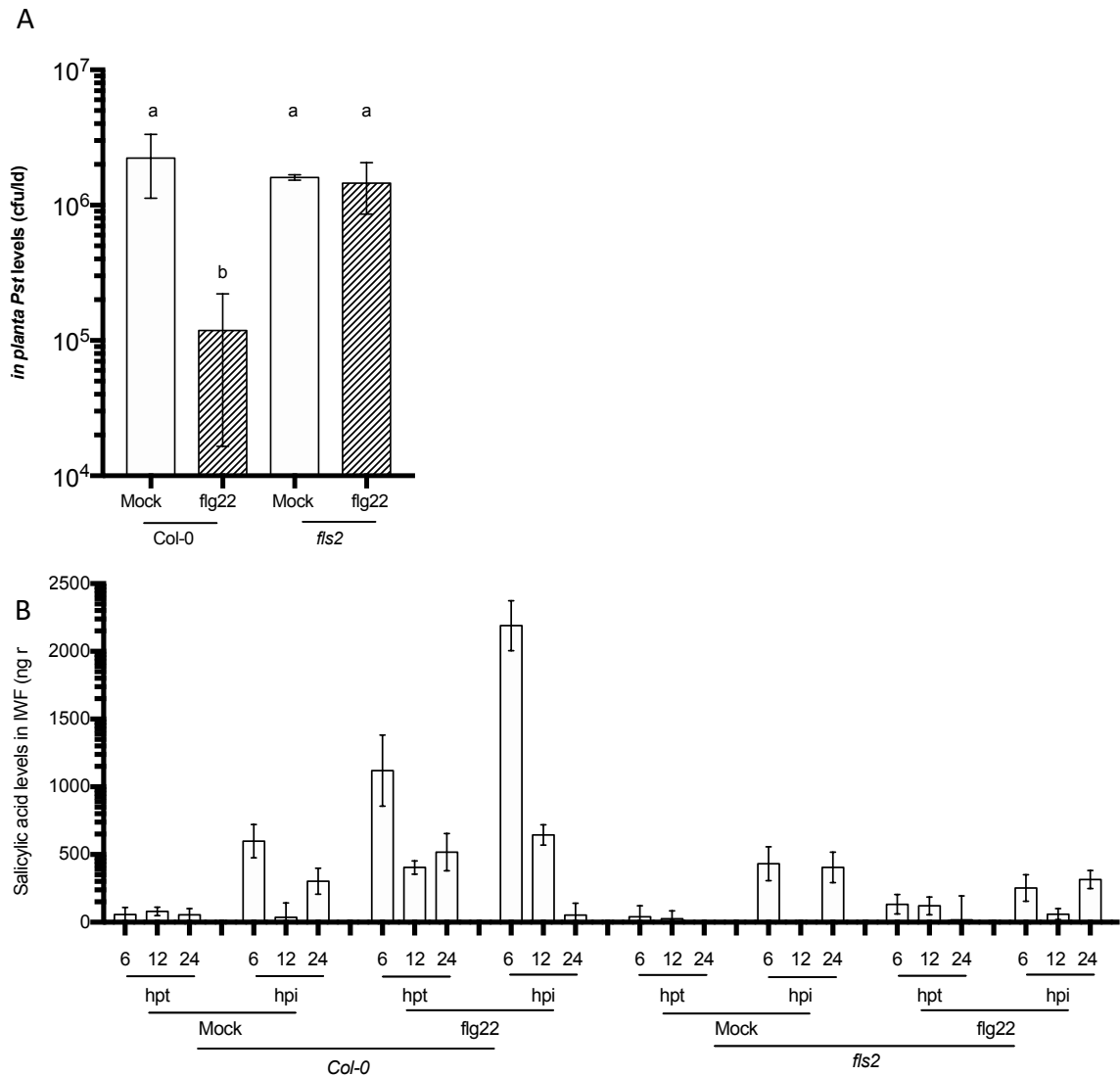


Figure 7. SA accumulates in intercellular washing fluids during PTI. A) Young (3.5 wpg) Col-0 and *fls2* plants were mock- or flg22-treated followed by *Pst* inoculation (10⁶ cfu/ml) 24 hours post treatment (hpt). *In planta* bacterial levels were measured at 72hpi. B) IWFs were collected at 6, 12, and 24 hours post treatment (hpt) and post inoculation (hpi). IWF SA levels were quantified using an SA biosensor assay. This experiment was repeated four times with similar results.

Chapter 4: Discussion and conclusions

4.1 *Pst* biofilm formation visualization

Biofilm formation by bacterial pathogens has been primarily studied in the human pathogens, *P. aeruginosa* and *Staphylococcus* species (reviewed by Joo and Otto, 2013) and more recently in plant-associated bacteria (reviewed by Bogino *et al.* 2013). Several studies examined plant-associated bacterial biofilm formation *in vitro* (Laue *et al.* 2006, Markel *et al.* 2016, Ude *et al.* 2006) using various methods such as scanning electron microscopy (Farias and Olmedilla 2019). In addition, only a few studies have shown aggregate formation of *Pst* during infection of plants such as Arabidopsis and tomato using fluorescence or electron microscopy (Whalen *et al.* 1991; Varvaro, Fanigliulo, and Babelegoto 1993; Badel *et al.* 2002; Boureau *et al.* 2002). Especially using electron scanning microscopy, *Pst* bacteria appears to form aggregates that encased in extracellular matrix *in vivo* (Whalen *et al.* 1991) and also *in vitro* (Farias and Olmedilla 2019). However, none of these studies examined the correlation of plant-associated bacterial aggregate formation to bacterial pathogenicity during plant infections. Furthermore, none of these studies further explored the makeup or the composition of the extracellular matrix encasing the bacterial aggregates. Overall, plant-associated bacterial aggregate formation has not been examined quantitatively in previous observations and there is no examination of the contribution to pathogenicity or the effect of defense on aggregate formation. To address this important gap of knowledge in this thesis, GFP-expressing *Pst*

biofilm-like aggregate formation was examined in susceptible and PTI-responding resistant *Arabidopsis* leaf intercellular spaces. As a result, *Pst* aggregate formation was positively associated with high bacterial growth *in planta*. To my knowledge, visualizing *Pst* biofilm-like aggregate formation *in vivo* has only been reported once by a previous lab member in leaves of susceptible young plants and ARR-responding mature plants (Wilson et al. 2017). To further explore the statistical correlation between aggregate formation and *Pst* pathogenicity, fields of view examined for each treatment group were doubled and aggregate size was determined to evaluate biofilm-like aggregate formation of different *Pst* strains in various environments. This quantitative approach can help us to distinguish the difference in aggregate formation when both *Pst* and *Pst* $\Delta algD \Delta algU \Delta mucAB$ formed aggregates but aggregates of *Pst* $\Delta algD \Delta algU \Delta mucAB$ appeared to be smaller than *Pst* aggregates in Col-0 leaves. As a result, aggregate formation was correlated with *Pst* pathogenicity *in planta*, suggesting biofilm formation contributes to *Pst* success. In addition to *Pst*, Godfrey *et al.* (2010) used *in vivo* confocal imaging to observe GFP-expressing *P. syringae* pv. *phaseolicola* (*Psp*) colony formation in inoculated bean leaves. They observed a reduction in bacterial colony formation in bean plants inoculated with an ETI-inducing avirulent strain of *Psp* compared to plants inoculated with a virulent bacteria strain, suggesting that suppression of bacterial aggregate formation may be part of the ETI response (Godfrey *et al.* 2010). To quantify aggregate formation, they examined 12 fields of view for three sections on one leaf and ImageJ was used to

quantify fluorescent pixels to represent aggregate formation during ETI-responding plants and susceptible plants quantitatively (Godfrey et al. 2010). However, they measured the total of green fluorescence signals in each field of view without considering number of aggregates and also the presence of fluorescent planktonic bacteria that are not in aggregates. The method used in this thesis helps us to obtain information how many aggregates are formed by *Pst* in leaves, and it also more accurately measures the size of the aggregates without accidentally including planktonic bacteria. The success in discovering the correlation between aggregate formation and bacterial success *in planta* led us to explore if *Pst* aggregates are *Pst* biofilms. If *Pst* aggregates are biofilms, aggregates should be encased in an extracellular matrix that contains polysaccharides, protein, DNA and lipids (Mann and Wozniak 2012).

In order to produce these biofilm components, *Pst* has to have essential genes for biofilm component biosynthesis. Using extracellular polysaccharides as examples, the *Pst* genome sequencing project revealed that *Pst* contains all the essential loci for synthesis of many extracellular polysaccharides, including cellulose, levan and alginate (Buell et al. 2003). Among these polysaccharides, cellulose and alginate were shown to be produced by *Pst in vitro* (Pérez-mendoza et al. 2019; Fett and Dunn 1989). Levan was detected and produced *in vitro* by *P. aeruginosa* (Strathmann, Wingender, and Flemming 2002) and *P. syringae pv. glycinea* (Osman et al. 1986; Laue et al. 2006). These polysaccharides (like cellulose, alginate and levan) contain alpha-(1,4) or beta-

(1,4) linkages between subunits, which can be detected by ConA or CFW staining, respectively (Strathmann, Wingender, and Flemming 2002; Laue et al. 2006; Mitra and Loqué 2014). It was hypothesized that *Pst* aggregates observed in this thesis are actually biofilms *in planta* and they should be surrounded by an extracellular matrix that contains polysaccharides and eDNA, both of which are common components of bacterial biofilms produced by some *Pseudomonas* bacteria (Mann and Wozniak 2012). eDNA DAPI signals were detected surrounding GFP-expressing *Pst* aggregates in leaf intercellular spaces. ConA and CFW signals were also observed to co-localize with GFP-expressing *Pst* aggregates in leaf intercellular spaces providing visual evidence that *Pst* aggregates may be embedded in a matrix of extracellular polysaccharides and eDNA and suggesting that *Pst* forms biofilms during infection of the leaf intercellular space. To my knowledge, this is the first data to provide evidence of *in vivo* co-localization of biofilm matrix components with bacterial aggregates in the leaf intercellular space during bacterial infection of *Arabidopsis*.

4.2 Functional alginate biosynthesis is important for biofilm-like aggregate formation, but not for growth of virulent *Pst* in *Arabidopsis*.

Some plant-associated bacteria (e.g. *P. fluorescens* & *P. putida*) form biofilm-like aggregates when they colonize plant root surfaces, preventing colonization by pathogens and enhancing plant resistance against pathogens (Couillerot et al. 2009; Espinosa-Urgel, Kolter, and Ramos 2002). However, some plant-associated bacteria (e.g. *Ralstonia solanacearum* and *Xanthomonas oryzae*)

form biofilm-like aggregates in plant intercellular spaces and are believed to produce biofilms and cause disease instead of providing benefits to plants (Wang et al. 2007; Kang et al. 2002). Biofilms appear to contribute to the bacterial success of both beneficial and pathogenic plant-associated bacteria mentioned above albeit in different environments.

In order to investigate the effect of biofilm formation on *Pst* success during *Arabidopsis* infection, the effect of alginate as a known biofilm component was examined. In this thesis, GFP-expressing *Pst* Δ *algD* growth and biofilm-like aggregate formation in *Arabidopsis* were examined to determine if the ability to produce alginate contributes to virulent *Pst* pathogenicity and biofilm-like aggregate formation. Wild-type *Arabidopsis* supported similarly high bacterial levels of *Pst* Δ *algD* and wild-type *Pst*, suggesting that functional alginate biosynthesis is not important for multiplication of virulent *Pst* in leaves. Ishiga et al. (2018) observed similar results in *Arabidopsis* and tomato plants inoculated with *algD* or wild-type *Pst*, suggesting the ability to produce alginate may be dispensable for growth of virulent *Pst* in *Arabidopsis*. These results were unexpected given that alginate is an important biofilm component of *P. aeruginosa* (Franklin et al. 2011) and *Pst* encodes alginate biosynthesis genes (Buell et al. 2003). Given that *Pst* Δ *algD* has a functional T3SS for effector secretion and produces the phytotoxin coronatine (Ishiga et al. 2018), both of which contribute to suppression of plant defenses such as PTI (Xin and He 2013), it is possible that alginate-containing biofilms are not necessary for *Pst*

multiplication and success *in planta*. Therefore, functional alginate biosynthesis may not be required when virulent *Pst* suppresses the plant PTI response in susceptible interactions.

Many extracellular polysaccharides are produced by bacteria forming biofilms during *in vitro* studies and it is thought that these extracellular polysaccharides promote immobilization of bacterial cells in the matrix, stabilize biofilm structures, and maintain attachment of bacteria to the surface of host cellular surfaces and protect the microbial community from host defense thus contributing to the pathogenicity of pathogens (Flemming and Wingender 2010; Flemming et al. 2016). However, it is not clear if the protection of plant-associated bacteria is achieved by producing extracellular polysaccharides and also if producing extracellular polysaccharides contributes to *Pst* biofilm formation *in vivo*. In this thesis, it was observed that during infection of *Arabidopsis* leaves, wild-type *Pst* formed more, and larger biofilm-like aggregates compared to *Pst* Δ *algD* that cannot produce alginate, providing evidence that alginate production is important for *Pst* biofilm-like aggregate formation *in planta*. To my knowledge, this is the first *in vivo* experiment that demonstrates that alginate biosynthesis contributes to *Pst* aggregate formation. There is *in vitro* evidence suggesting that the ability to produce alginate contributes to biofilm formation of some *Pseudomonas* species. For example, human chronic pulmonary infections are associated with *P. aeruginosa* strains that produce alginate. Additionally, alginate is commonly produced in *P. aeruginosa* isolated from cystic fibrosis patients and not produced

in isolates from other environments, suggesting that alginate production is important for *P. aeruginosa* biofilm formation in humans (Muhammadi and Ahmed 2007; Hoiby, Ciofu, and Bjarnsholt 2010). In *P. syringae*, a *Pss* quorum sensing mutant that is defective for production of the AHL quorum sensing signal, was shown to produce little alginate and was more susceptible to hydrogen peroxide treatment *in vitro*, suggesting that alginate production is important for bacterial tolerance of reactive oxygen species (ROS) (Quiñones, Dulla, and Lindow 2005). ROS (e.g. hydrogen peroxide) are important signaling and antimicrobial molecules that accumulate during PTI (Bigeard, Colcombet, and Hirt 2015; Zipfel 2009), thus alginate production may contribute to protection of *Pseudomonas* bacteria from ROS-producing plant immune responses like PTI. In addition, the *Pss* quorum sensing mutant did not cause visible lesions in bean pods, unlike wild-type *Pss*, suggesting that in the absence of alginate production, *Pss* is negatively impacted in causing disease, suggesting that the ability to produce alginate may be involved in *Pseudomonas* pathogenicity. (Quiñones, Dulla, and Lindow 2005). Laue *et al.* (2006) investigated the roles of alginate and levan in *Pseudomonas syringae* pv. *glycinea* (*Psg*) biofilm formation *in vitro*. Strains deficient in the production of the extracellular polysaccharide alginate or the exopolysaccharide levan, or deficient in both, formed biofilms on polystyrene surfaces (Laue et al, 2006), providing evidence that the ability to produce alginate and levan are not essential for *Psg* to form biofilm *in vitro*. This may seem contradictory to the results in this thesis, however, bacteria under *in vitro*

conditions are not exposed to plant-produced molecules such as SA and reactive oxygen species, which are found to change bacterial behaviours to respond to antimicrobial stress (Subramoni et al. 2014; Li et al. 2020). Thus, *P. syringae* may form biofilms differently in different environments. More importantly, there are no plant-produced antibiofilm agents in *in vitro* assays, therefore producing alginate- and/or levan-containing biofilm may not be important for bacterial success. In this thesis, there were no differences observed in multiplication of *Pst* and *Pst ΔalgD* *in planta*, suggesting that forming alginate-containing biofilms may not be necessary for *Pst* multiplication *in planta* because *Pst ΔalgD* has a functional T3SS for effector secretion and produces the phytotoxin coronatine (Ishiga et al. 2018), both of which contribute to suppression of plant defenses such as PTI (Xin and He 2013). Taken together, this thesis is the first attempt to examine the impact of alginate production on *Pst* aggregate formation *in vivo* and provides novel evidence that functional alginate biosynthesis is important for aggregate formation, but not for growth of virulent *Pst* in *Arabidopsis*.

4.3 Biofilm-like aggregate formation contributes to *Pst* pathogenicity

Since the *Pst ΔalgD* grew as well as wild-type *Pst* indicating that *Pst ΔalgD* is similarly virulent to wild-type *Pst* in *Arabidopsis*, a *Pst* strain with reduced virulence was needed to investigate biofilm-like aggregate formation and its association with bacterial success. *Pst ΔalgD ΔalgU ΔmucAB* displayed reduced virulence and a reduced ability to suppress plant defense in addition to its inability to produce alginate because many T3SS genes are not unregulated (Markel et al.

2016). This is due to the fact that *AlgU* encodes the alternative sigma factor AlgU, which regulates its own expression, the alginate biosynthetic operon, as well as other T3SS regulatory genes such as HrpL (Markel et al. 2016). In addition, MucA and MucB are anti-sigma factors that form a complex with AlgU to inactivate AlgU (Bao et al. 2020). Tomato infection assays suggest that AlgU function is important for *in planta* bacterial multiplication and disease (Markel et al. 2016). It has been demonstrated in several studies that virulent *Pst* forms biofilm-like aggregates in *Arabidopsis* and tomato leaves, however without examining the contribution of aggregate formation to pathogenicity of plant-associated bacteria (Whalen et al. 1991; Varvaro, Fanigliulo, and Babelegoto 1993; Badel et al. 2002; Boureau et al. 2002). In this thesis, it was demonstrated that the *Pst* $\Delta algD \Delta algU \Delta mucAB$ displayed reduced bacterial multiplication in *Arabidopsis* leaves compared to wild-type *Pst*, indicating that *Pst* $\Delta algD \Delta algU \Delta mucAB$ displayed reduced pathogenicity and was less successful. In addition, *Pst* $\Delta algD \Delta algU \Delta mucAB$ formed fewer and smaller aggregates compared to wild-type *Pst* in *Arabidopsis* leaves, suggesting that plant defense was highly effective in suppressing *Pst* $\Delta algD \Delta algU \Delta mucAB$ bacterial multiplication and aggregate formation. Since *Pst* $\Delta algD$ grew to similar levels as wild-type *Pst* in *Arabidopsis* and MucAB down-regulates *AlgU* expression (Bao et al. 2020), this leads to the suggestion that *AlgU* function is important for pathogenicity of *Pst* *in planta* and AlgU promotes *Pst* success in *Arabidopsis*. This is consistent with a study by Markel et al. (2016), in which *Pst* $\Delta algU \Delta mucAB$ displayed a reduced

ability to cause necrosis and chlorosis and complementation of *Pst ΔalgU ΔmucAB* with an *AlgU*-overexpressing vector resulted in increased necrotic spots and chlorosis compared to wild-type *Pst* in tomato leaves. Transcriptome analysis of *Pst ΔalgU ΔmucAB* with the *AlgU* over-expression vector compared to *Pst ΔalgU ΔmucAB* with the control vector, revealed that 38% of HrpL-upregulated genes were under AlgU control. HrpL is a sigma factor responsible for controlling expression of the Hrp system, which includes the T3SS and effectors, some of which suppress plant immune responses and promote disease in plants (Fouts et al. 2002). The set of genes upregulated by both AlgU and HrpL includes functions involved in regulation of transcription (*HrpL* and *SigX*), post-translational regulation of the Hrp system expression (*HrpV*), structural genes for the T3SS apparatus (*HrcC* and *HrcQb*), and T3SS substrates that include the pilus protein gene (*HrpA1*) and PTI-suppressing effectors (*HopY1*, *AvrPtoB*, *AvrPto*, and *HopE1*) (Markel et al. 2016). Therefore, these results support the idea that *Pst* AlgU contributes to plant immune suppression by regulating the T3SS, and to bacterial pathogenicity by regulating the alginate biosynthesis operon.

In addition, AlgU was found to downregulate flagellin gene expression, which may allow *Pst* to avoid flagellin-mediated PTI detection. Downregulation of flagellin gene expression may also promote the switch from planktonic to sessile bacterial cells to initiate formation of biofilms during infection (Bao et al. 2020). This idea is consistent with the results presented in this thesis, in which *Pst ΔalgD ΔalgU ΔmucAB* formed few aggregates compared to many aggregates of

wild-type *Pst* in *Arabidopsis* leaves. This suggests that AlgU function is required for biofilm formation by regulating alginate production and promoting the switch from planktonic to sessile bacterial cells by downregulating flagellin gene expression. Because PTI responses begin with the recognition of PAMPs such as flagellin, AlgU-mediated downregulation of flagellin may result in reduced PAMP recognition and thus reduced PTI responses.

Plant pathogens have evolved mechanisms to evade PTI detection and actively suppress plant immune responses (Mohan et al. 2018). Biofilm formation signaling events may also contribute to *Pst* success *in planta* by helping bacteria evade PTI detection. For example, when bacterial flagellin is detected, it initiates the PTI response in *Arabidopsis*. Thus, reducing flagellin expression may contribute to aggregate formation as cells are generally tightly packed and immobile in aggregates and reducing flagellin expression may be beneficial as it reduces bacterial recognition by the plant. In order to reduce flagellin expression, bacteria use Bis-(3'-5')-cyclic dimeric guanosine monophosphate (c-di-GMP) as a ubiquitous bacterial secondary messenger to contribute to flagellin expression downregulation to control the molecular decision of existing as planktonic motile cells versus sedentary aggregated bacterial cells (Hengge 2009). High c-di-GMP levels are generally associated with reduced expression and/or activity of flagella and enhanced expression of various adhesins and biofilm-associated exopolysaccharides in some bacteria like *P. aeruginosa* and *Pst* (Hengge 2009). Engl et al. (2014) first described the importance of biofilm formation and immune

evasion in relation to the ability to produce c-di-GMP in *Pst*. The ability to make bacterial signal c-di-GMP in *Pst* was found to promote biofilm formation *in vitro* (Engel et al. 2014). It was also observed that *Arabidopsis* was able to accumulate SA in leaves when leaves were inoculated with a c-di-GMP biosynthesis mutant, *Pst* Δ *chp8* that cannot down regulate flagellin expression, suggesting that reducing flagellin expression contributes to bacterial evasion of PTI *in vivo* (Engl et al. 2014). When *Pst* is exposed to the flavonoid phloretin *in vitro*, it activates Chp8, a *Pseudomonas* diguanylate cyclase enzyme, that synthesizes c-di-GMP (Vargas et al. 2013). c-di-GMP then signals planktonic bacterial cells to enter a sessile biofilm phase by repressing flagellin production and promoting EPS production *in vitro*, however, *Pst* Δ *chp8* aggregates or biofilm formation in leaves was not examined using microscopy in Engl et al. (2014). Based on several studies investigating the role of AlgU during *Pseudomonas* infection of plants (Markel et al. 2016; Markel et al. 2018; Ishiga et al. 2018; Bao et al. 2020), AlgU and Chp8 produce similar signaling outcomes in *Pst*, where both promote the retraction of flagella and suppression of flagellar protein synthesis. It is believed that down regulation of flagellar protein expression allows *Pseudomonas* to avoid detection by the PTI machinery. Thus, biofilm formation may also contribute to bacterial success via reducing/masking immunogenic PAMPs like flagellin. This is consistent with the results in this thesis where we demonstrated the correlation of aggregate formation in leaves and bacterial success *in planta*. Most importantly, these data suggest that *Pst* may evade PTI during biofilm-like aggregate

formation. It may affect bacterial pathogenicity and success *in planta* if PTI prevents biofilm-like aggregate formation.

4.4 PTI suppresses biofilm-like aggregate formation & bacterial success in an SA-dependent manner *in vivo*

Wilson et al. (2017) observed that *Pst* formed few aggregates in ARR-competent plants, whereas many aggregates were observed in young susceptible plants, suggesting that suppression of *Pst* biofilm-like aggregate formation is an important component of the ARR response. This thesis expanded on this work to determine if suppression of biofilm-like aggregate formation is also an important component of the PTI response, which might suggest that suppression of biofilm-like aggregate formation is a shared mechanism among plant immune responses. Wild-type *Pst* formed large aggregates in susceptible plants including in *fls2* mutants that are unable to initiate flg22-mediated PTI, while few aggregates were observed in PTI-responding plants, suggesting that PTI induced by flg22 treatment suppresses *Pst* biofilm-like aggregate formation. This is a novel finding that demonstrates that PTI involves suppression of *Pst* biofilm-like aggregate formation, leading to the idea that suppression of biofilm-like aggregate formation is a component in plant immune responses.

Wilson et al (2017) provide compelling evidence that SA acts as an antimicrobial and antibiofilm agent during ARR. Thus, the effect of SA on biofilm-like aggregate formation during PTI was explored. If plant-produced SA acts as an antimicrobial and antibiofilm agent during PTI like it does during ARR, *Pst*

ΔalgD ΔalgU ΔmucAB should display improved bacterial success and aggregate formation in SA-defective plants compared to wild-type plants. As expected, *Pst ΔalgD ΔalgU ΔmucAB* bacterial levels increased by ~100 fold in *sid2-2* leaves compared to wild-type Col-0 leaves, suggesting that plant-produced SA negatively affected *Pst ΔalgD ΔalgU ΔmucAB* multiplication and success in wild-type Col-0 leaves. In addition, *Pst ΔalgD ΔalgU ΔmucAB* formed no large aggregates and few small aggregates in wild-type SA-producing leaves but formed many large aggregates in SA-defective *sid2-2* leaves, similar to wild-type *Pst* in *sid2-2* leaves. These results provide evidence that plant-produced SA is involved in suppressing biofilm-like aggregate formation. The effect of SA in suppressing aggregate formation was also demonstrated using SA hyperaccumulating *Arabidopsis* mutant (*lox2* and *cpr5-2*) roots interacting with *P. aeruginosa*. *P. aeruginosa* biofilm-like aggregates were observed on SA hyperaccumulating mutant root surfaces as detected by Calcofluor white staining, whereas larger biofilm-like aggregates were observed on wild-type plant roots (Prithiviraj, Bais, et al. 2005). These data suggest that SA accumulation may contribute to plants defense against biofilm-like aggregate forming bacteria. However, it is still unclear how SA accumulation achieves these effects on aggregate formation in plants, except intercellular SA accumulations during age-related resistance in *Arabidopsis* (Wilson et al. 2017).

4.5 During PTI SA accumulates in leaf intercellular spaces and is associated with suppression of *Pst* multiplication and biofilm-like aggregate formation *in vivo*

Given that Wilson et al. (2017) provides evidence that intercellular SA acts as an antimicrobial and antibiofilm agent during ARR, along with the data in this thesis that supports a role for SA in the suppression of biofilm-like aggregate formation during PTI, this led us to examine if SA also accumulates in leaf intercellular washing fluids (IWFs) collected during PTI. Flg22-treated PTI-responding Col-0 leaves accumulated high levels of SA in IWFs collected from leaves in which few aggregates were observed. Additionally, mock-treated susceptible plants (Col-0 and *fls2*) accumulated little SA in IWFs collected from leaves in which many large *Pst* aggregates were observed, suggesting that SA accumulates in leaf intercellular spaces. Moreover, intercellular accumulation of SA is associated with reduced *Pst* multiplication and biofilm-like aggregate formation during PTI. To my knowledge, this is the first demonstration that SA accumulates in the intercellular space during PTI and is associated with a negative impact on bacterial success and biofilm-like aggregate formation *in vivo*. In mature plants during Age-Related Resistance (ARR), accumulation of SA in leaf intercellular spaces of *Arabidopsis* is observed in response to *Pst* infection, but not in young susceptible (3-4 wpg) plants (Cameron and Zaton 2004; Carviel et al. 2009; Wilson et al. 2017) consistent with the results in young (3-4 wpg) plants in this thesis. In addition, IWFs collected from mature plants inoculated

with *Pst* often inhibit *Pst* growth *in vitro* and reduction of SA in leaf intercellular spaces by infiltrating salicylate hydroxylase into ARR-competent plants resulted in a reduced ARR response. Conversely, infiltrating SA into the intercellular space rescued ARR-defective mutants and enhanced ARR in wild-type Col-0 (Cameron and Zaton 2004). Altogether, these data suggest that SA acts as an antimicrobial and antibiofilm agent in leaf intercellular spaces during ARR. In Wilson et al. 2017, the reduction of bacterial success and also accumulation of SA with a concentration peaked at 2000ng ml IWF⁻¹ in leaf intercellular spaces of mature ARR plants. The concentration of SA in IWFs collected from PTI-responding plants was similar to ARR-competent plants peaking at ~2000ng ml IWF⁻¹. Bacterial success and also aggregate formation of *Pst* were reduced in PTI-responding leaves that accumulates SA in leaf intercellular spaces similarly to observations in ARR plants, suggesting that SA also plays an antimicrobial and antibiofilm role in leaf intercellular spaces during PTI as well. Taken together, and data in this thesis demonstrates that SA plays a similar role in PTI as it does in ARR. Furthermore, high levels of intercellular SA accumulated in ETI-responding plants inoculated with *Pst avrRpt2*, suggesting that intercellular SA accumulation also contributes to ETI (Carviel et al. 2014). Overall, this thesis and the studies discussed above provide compelling evidence that SA acts as an antimicrobial and antibiofilm agent in leaf intercellular spaces during PTI, ETI and ARR.

Intercellular SA may also have a role in suppressing bacterial quorum sensing. For example, during *Agrobacterium* infection of plants, plant-produced

SA is believed to serve a quorum-quenching role as *Agrobacterium* dampens its quorum sensing signals in an SA-dependent manner and *Agrobacterium* virulence gene expression is reduced hinting that SA has a direct effect on *Agrobacterium* and potentially influence its virulence (Subramoni et al. 2014). Earlier studies identified SA as a modulator of virulence in human pathogenic *P. aeruginosa in vitro* (Bandara et al. 2006) and SA concentrations of 1.5 mM were found to suppress an array of quorum sensing-related gene expressions in *P. aeruginosa* growing in culture (Yang et al. 2009). SA concentrations that are greater than 1.8 mM have also been shown to suppress biofilm generation in *E. coli* grown in culture (Cattò et al. 2017). More recently, SA was identified in a screen for AHL synthase inhibitors (Chang et al. 2014), suggesting that SA can directly target quorum sensing signal production and possible downstream pathogenicity and biofilm responses in *E. coli* and *P. aeruginosa*. Thus, a number of studies support the idea that SA modulates biofilm formation in a number of ways, including interfering with quorum sensing signaling.

4.6 – Conclusions and novel contributions to knowledge

This thesis provides compelling evidence that *in planta Pst* biofilm-like aggregates are encased in an extracellular matrix containing eDNA and polysaccharides and are biofilms. Evidence that alginate is a contributor to *Pst* biofilm-like aggregate formation *in vivo* was also provided. Furthermore, I demonstrated that *Pst* success during infection of *Arabidopsis* is associated with *Pst's* ability to form biofilm-like aggregate *in vivo*. Quantitative evidence that

plant-produced SA negatively affects the size and number of *Pst* biofilm-like aggregates that form in planta, was provided. Moreover, intercellular SA accumulated during PTI, but not during susceptible interactions indicating that intercellular SA accumulation is associated with reduced bacterial success and suppression of biofilm-like aggregate formation in leaves. Taken together, this thesis provides compelling evidence that SA acts as an antimicrobial and antibiofilm agent in leaf intercellular spaces during PTI supporting the idea that SA accumulation in leaf intercellular spaces is a common component of plant immune responses (ETI, PTI, ARR) by suppressing bacterial biofilm formation and bacterial success. In conclusion, I contributed to understanding of the role of *Pst* biofilm formation during infection which is not well studied. In addition, I have contributed to advancing our understanding of the PTI response in terms of suppression of bacterial biofilm formation. This knowledge could potentially be used to enhance disease resistance in economically valuable crops in the future.

4.7 Future Directions

While this thesis provides compelling evidence that supports my hypotheses, it also leads to new ideas for further investigation.

1. In this thesis, it was observed that SA accumulated in PTI-responding resistant plants, suggesting that SA plays an antimicrobial and antibiofilm role in leaf intercellular spaces because bacterial multiplication and biofilm-like aggregate formation were reduced in these plants. Additional evidence

of the antimicrobial and antibiofilm activities of SA in leaf intercellular spaces could be obtained by:

- A. Determining if SA-containing IWFs collected from PTI-responding leaves suppress bacterial growth and biofilm formation *in vitro*.
- B. Determining if the SA-deficient *sid2-2* and *fls2* PTI-defective plants can be rescued in terms of suppressing *Pst* multiplication and biofilm-like aggregate formation by adding SA into the intercellular space before inoculation with wild-type *Pst*.

2. The PTI response is the result of complex signaling cascades after plant receptors recognize PAMPs of bacterial pathogens. However, some signaling steps leading to intercellular accumulation of SA have not been identified. Therefore, it would be an important contribution to our understanding of this important plant immune response to elucidate how the PTI signaling pathway leads to accumulation of SA in leaf intercellular spaces. To contribute to understanding what initiates SA accumulation during PTI, I collected samples from PTI-responding and susceptible leaves and performed total RNA extractions. The RNA samples were sent to a sequencing facility (GeneWiz in New Jersey, US) for quality check analysis and sequencing. For Quality check analysis, see more details in Figure A1.

3. In addition to elucidating how PTI signaling results in intercellular SA accumulation, it has been shown that intercellular SA accumulation occurs during ARR (Wilson et al. 2017) and also ETI (Carviel et al. 2014). If transcriptomes can be obtained from ARR-responding and ETI-responding plants when intercellular SA accumulation occurs, it may be possible to identify the unknown transporter protein(s) responsible for transporting SA into the intercellular space as this transporter should be upregulated during all these plant immune responses. In addition, by comparing these transcriptomes, it may also be possible to identify shared genes which play a common, but significant role in these plant defense responses.

4. In order to further investigate if biofilm-like aggregates observed in leaf intercellular spaces are actually biofilms, more biofilm-biosynthesis mutant *Pst* should be examined for biofilm matrix components during infection of *Arabidopsis* using the staining protocol in this thesis. Because there are extracellular macromolecules (like polysaccharides, proteins, DNA and lipids) produced by plants. The staining data in this thesis cannot identify the origin of the extracellular polysaccharides and eDNA in the matrix around *Pst* aggregates *in planta*. It is possible that some of the signals we thought were polysaccharides or eDNA produced by plants instead of bacteria. If the signals or some signals we observed in this thesis works

were bacterial-origin, staining of biofilm-biosynthesis mutant *Pst* biofilms should display no signals or reduced signals for eDNA and/or polysaccharides. In that case, it will provide strong evidence to indicate that aggregates are embedded in a extracellular matrix that produced by bacteria during biofilm formation.

Appendix A

Figure A1 – PTI RNA Quality Check Analysis

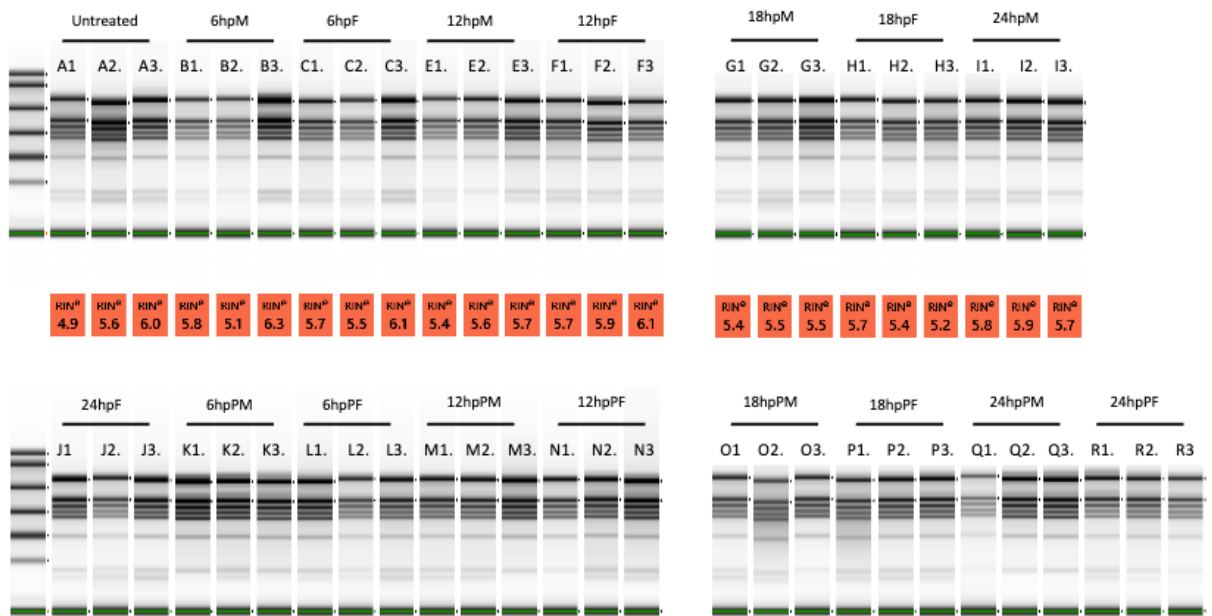


Figure A1. Quality check analysis of PTI total RNA samples. Young (3.5 wpg) Col-0 plants were mock- or flg22-treated followed by wild-type *Pst* inoculation (10^6 cfu/ml) at 24 hours post treatment. *In planta* bacterial levels were measured at 72 hours post inoculation. IWFs were collected from untreated leaves and treated leaves at 6,12,18 and 24 hours post treatment, mock-treated (hpM) or flg22-treated (hpF). IWFs were also collected from treated and inoculated leaves at 6, 12, 18 and 24 hours post inoculation, mock-treated (hpPM) or flg22-treated (hpPF).

All total RNA samples presented in the figure A1 passed the quality check analysis and were sequenced by GeneWiz. The total transcriptome data are now available for differential expression analysis to elucidate PTI signaling pathways that are responsible for intercellular SA accumulation during PTI.

Table A1 – PTI response suppresses bacterial levels *in planta*

Genotype	Treatment	Bacterial Levels <i>in planta</i> (cfu/l) ¹							
		1	2	3	4	5	6	7	8
Col-0	mock	1.60x10 ⁶	3.73x10 ⁶	5.27x10 ⁶	1.85x10 ⁶	7.50x10 ⁶	7.09x10 ⁵	5.40x10 ⁶	8.44x10 ⁶
	flg22	5.00x10 ⁴	1.73x10 ⁵	5.29x10 ⁴	3.56x10 ⁴	1.11x10 ⁵	7.56x10 ⁴	3.44x10 ⁴	1.00x10 ⁶
<i>fls2</i>	mock	3.42x10 ⁵	1.67x10 ⁶	3.90x10 ⁶	1.69x10 ⁶	3.38x10 ⁶	5.21x10 ⁵	1.25x10 ⁶	6.07x10 ⁵
	flg22	5.88x10 ⁵	1.25x10 ⁶	3.35x10 ⁶	6.46x10 ⁵	3.94x10 ⁶	1.25x10 ⁶	1.46x10 ⁶	5.52x10 ⁶
<i>sid2-2</i>	mock	1.50x10 ⁶	3.15x10 ⁶	7.23x10 ⁶	2.56x10 ⁶	1.10x10 ⁷	9.81x10 ⁶	9.79x10 ⁶	5.40x10 ⁶
	flg22	1.23x10 ⁶	4.58x10 ⁵	4.58x10 ⁵	3.75x10 ⁵	2.27x10 ⁶	8.29x10 ⁶	1.94x10 ⁶	7.51x10 ⁵

¹ Leaves were infiltrated with water (mock-treated) or 1 μM flg22 (flg22-treated), 24 hours later, the same leaves were inoculated with virulent GFP-expressing *Pst*. *In planta* bacterial levels were determined at 72 hpi. The fold differences are calculated as the bacterial level in mock-treated group divided by the bacterial level in flg22-treated group in each genotype and each experiment. PTI responses was the statistically significant fold difference in *Pst* levels (cfu/l). See calculated statistically significant fold difference in *Pst* levels in Table 1.

Reference

Afzal, Ahmed J, and David Mackey. 2011. "Separable Fragments and Membrane Tethering of Arabidopsis RIN4 Regulate Its Suppression of PAMP-Triggered Immunity." *The Plant Cell* 23: 3798–3811.

<https://doi.org/10.1105/tpc.111.088708>.

Agrios, George N. 2005. *Plant Pathology*.

Amborabé, Bénigne Ernest, Pierrette Fleurat-Lessard, Jean François Chollet, and Gabriel Roblin. 2002. "Antifungal Effects of Salicylic Acid and Other Benzoic Acid Derivatives towards *Eutypa Lata*: Structure-Activity Relationship." *Plant Physiology and Biochemistry* 40 (12): 1051–60.

[https://doi.org/10.1016/S0981-9428\(02\)01470-5](https://doi.org/10.1016/S0981-9428(02)01470-5).

Arnold, Dawn L, and Gail M Preston. 2019. "Pseudomonas Syringae : Enterprising Epiphyte and Stealthy Parasite." *Microbiology* 165: 251–53.

<https://doi.org/10.1099/mic.0.000715>.

Aslam, Shazia N., Mari Anne Newman, Gitte Erbs, Kate L. Morrissey, Delphine Chinchilla, Thomas Boller, Tina Tandrup Jensen, et al. 2008. "Bacterial Polysaccharides Suppress Induced Innate Immunity by Calcium Chelation." *Current Biology* 18 (14): 1078–83. <https://doi.org/10.1016/j.cub.2008.06.061>.

Badel, J. L., A. O. Charkowski, W. L. Deng, and A. Collmer. 2002. "A Gene in the Pseudomonas Syringae Pv. Tomato Hrp Pathogenicity Island Conserved Effector Locus, HopPtoA1, Contributes to Efficient Formation of Bacterial

Colonies in Planta and Is Duplicated Elsewhere in the Genome.” *Molecular Plant-Microbe Interactions* 15 (10): 1014–24.

<https://doi.org/10.1094/MPMI.2002.15.10.1014>.

Baker, C Jacyn, Natalia Y Kovalskaya, Norton M Mock, Robert A Owens, Kenneth L Deahl, Bruce D Whitaker, Daniel P Roberts, Rose W Hammond, and Andrey A Aver. 2012. “Physiological and Molecular Plant Pathology An Internal Standard Technique for Improved Quantitative Analysis of Apoplastic Metabolites in Tomato Leaves.” *Physiological and Molecular Plant Pathology* 78 (2012): 31–37. <https://doi.org/10.1016/j.pmpp.2012.01.001>.

Bandara, Mahesh B K, Hua Zhu, Padmaja R Sankaridurg, and Mark D P Willcox. 2006. “Salicylic Acid Reduces the Production of Several Potential Virulence Factors of *Pseudomonas Aeruginosa* Associated with Microbial Keratitis.” *Investigative Ophthalmology & Visual Science* 47 (10): 4453–60. <https://doi.org/10.1167/iovs.06-0288>.

Bao, Zhongmeng, Hai-Lei Wei, Xing Ma, and Bryan Swingle. 2020. “*Pseudomonas Syringae* AlgU Downregulates Flagellin Gene Expression, Helping Evade Plant Immunity” 202 (4): 1–11.

Bigeard, Jean, Jean Colcombet, and Heribert Hirt. 2015a. “Signaling Mechanisms in Pattern-Triggered Immunity (PTI).” *Molecular Plant* 8: 521–39. <https://doi.org/10.1016/j.molp.2014.12.022>.

Block, Anna, Eric Schmelz, Jeffery B. Jones, and Harry J. Klee. 2005.

- “Coronatine and Salicylic Acid: The Battle between Arabidopsis and Pseudomonas for Phytohormone Control.” *Molecular Plant Pathology* 6 (1): 79–83. <https://doi.org/10.1111/J.1364-3703.2004.00265.X>.
- Bogino, Pablo C, María De, Mercedes Oliva, and Fernando G Sorroche. 2013. “The Role of Bacterial Biofilms and Surface Components in Plant-Bacterial Associations.” *Int.J.Mol.Sci*, 2013. <https://doi.org/10.3390/ijms140815838>.
- Boller, Thomas, and Georg Felix. 2009. “A Renaissance of Elicitors: Perception of Microbe-Associated Molecular Patterns and Danger Signals by Pattern-Recognition Receptors.” *Annual Review of Plant Biology* 60 (1): 379–406. <https://doi.org/10.1146/annurev.arplant.57.032905.105346>.
- Bolund, P, and S Hunhammar. 1999. “Ecosystem Services in Urban Areas.” *Ecological Economics* 29 (2): 293–301. [https://doi.org/10.1016/S0921-8009\(99\)00013-0](https://doi.org/10.1016/S0921-8009(99)00013-0).
- Boureau, Tristan, Jarkko Routtu, Elina Roine, Suvi Taira, and Martin Romantschuk. 2002. “Localization of HrpA -Induced Pseudomonas Syringae Pv. Tomato DC3000 in Infected Tomato Leaves.” *Molecular Plant Pathology* 3 (6): 451–60.
- Brown, Darby G, Jill K Swanson, and Caitilyn Allen. 2007. “Two Host-Induced Ralstonia Solanacearum Genes, AcrA and DinF, Encode Multidrug Efflux Pumps and Contribute to Bacterial Wilt Virulence.” *Applied and Environmental Microbiology* 73 (9): 2777–86. <https://doi.org/10.1128/AEM.00984-06>.

- Buell, C Robin, Vinita Joardar, Magdalen Lindeberg, Jeremy Selengut, Ian T Paulsen, Michelle L Gwinn, Robert J Dodson, et al. 2003. "The Complete Genome Sequence of the Arabidopsis and Tomato Pathogen *Pseudomonas Syringae* Pv . Tomato DC3000." *PNAS* 100 (18).
- Buttner, Daniela, and Sheng Yang He. 2009. "Type III Protein Secretion in Plant Pathogenic Bacteria." *Plant Physiology* 150: 1656–64.
<https://doi.org/10.1104/pp.109.139089>.
- Cameron, Robin K., and Kasia Zaton. 2004. "Intercellular Salicylic Acid Accumulation Is Important for Age-Related Resistance in Arabidopsis to *Pseudomonas Syringae*." *Physiological and Molecular Plant Pathology* 65 (4): 197–209. <https://doi.org/10.1016/J.PMPP.2005.02.002>.
- Carr, John P, Roger N Beacw, and Daniel F Klessig. 1989. "Are the PR1 Proteins of Tobacco Involved in Genetically Engineered Resistance to TMV ?" *Virology* 169: 470–73.
- Carviel, Jessie L, Fadi Al-daoud, Melody Neumann, Asif Mohammad, Nicholas J Provar, Wolfgang Moeder, Keiko Yoshioka, and Robin K Cameron. 2009. "Forward and Reverse Genetics to Identify Genes Involved in the Age-Related Resistance Response in Arabidopsis Thaliana." *Molecular Plant Pathology* 10 (5): 621–34. <https://doi.org/10.1111/J.1364-3703.2009.00557.X>.
- Carviel, Jessie L, Daniel C Wilson, Marisa Isaacs, Philip Carella, Vasile Catana,

- Brian Golding, Elizabeth A Weretilnyk, and Robin K Cameron. 2014. "Investigation of Intercellular Salicylic Acid Accumulation during Compatible and Incompatible Arabidopsis- Pseudomonas Syringae Interactions Using a Fast Neutron-Generated Mutant Allele of EDS5 Identified by Genetic Mapping and Whole-Genome Sequencing." *PLoS ONE* 9 (3): e88608. <https://doi.org/10.1371/journal.pone.0088608>.
- Cattò, Cristina, Giovanni Grazioso, Silvia Dell Orto, Arianna Gelain, Valeria Marzano, Alberto Vitali, Federica Villa, et al. 2017. "The Response of Escherichia Coli Biofilm to Salicylic Acid." *Biofouling* 33 (3): 235–51. <https://doi.org/10.1080/08927014.2017.1286649>.
- Cava, Joseph R, Pappi M Elias, Debra A Turowski, and K Dale Noel Noel. 1989. "Rhizobium Leguminosarum CFN42 Genetic Regions Encoding Lipopolysaccharide Structures Essential for Complete Nodule Development on Bean Plants." *Journal of Bacteriology* 171 (1): 8–15.
- Chang, Chien-yi, Thiba Krishnan, Hao Wang, Ye Chen, Wai-fong Yin, and Yee-meng Chong. 2014. "Non-Antibiotic Quorum Sensing Inhibitors Acting against N -Acyl Homoserine Lactone Synthase as Druggable Target." *Scientific Reports* 4 (7245): 1–8. <https://doi.org/10.1038/srep07245>.
- Chatterjee, Asita, Yaya Cui, Hiroaki Hasegawa, and Arun K Chatterjee. 2007. "PsrA , the Pseudomonas Sigma Regulator , Controls Regulators of Epiphytic Fitness , Quorum-Sensing Signals , and Plant Interactions in Pseudomonas Syringae Pv . Tomato Strain DC3000." *Applied and*

Environmental Microbiology 73 (11): 3684–94.

<https://doi.org/10.1128/AEM.02445-06>.

Chinchilla, Delphine, Zsuzsa Bauer, Martin Regenass, Thomas Boller, and Georg Felix. 2006. “The Arabidopsis Receptor Kinase FLS2 Binds Flg22 and Determines the Specificity of Flagellin Perception.” *The Plant Cell* 18 (February): 465–76. <https://doi.org/10.1105/tpc.105.036574.1>.

Chitnis, Chetan E, and Dennis E Ohman. 1993. “Genetic Analysis of the Alginate Biosynthetic Gene Cluster of *Pseudomonas Aeruginosa* Shows Evidence of an Operonic Structure.” *Molecular Microbiology* 8 (3): 583–90.

Choi, Jaeyoung, Ki-Tae Kim, Jongbum Jeon, and Yong-Hwan Lee. 2013. “Fungal Plant Cell Wall-Degrading Enzyme Database: A Platform for Comparative and Evolutionary Genomics in Fungi and Oomycetes.” *BMC Genomics* 14 (Suppl 5): S7. <https://doi.org/10.1186/1471-2164-14-S5-S7>.

Clifford, Jennifer C, Jeannette N Rapicavoli, and M Caroline Roper. 2013. “A Rhamnose-Rich O-Antigen Mediates Adhesion , Virulence , and Host Colonization for the Xylem-Limited Phytopathogen *Xylella Fastidiosa*.” *MPMI* 26 (6): 676–85.

Costerton, J W, Philip S Stewart, and E P Greenberg. 1999. “Bacterial Biofilms : A Common Cause of Persistent Infections.” *Science* 284: 1318–23.

Couillerot, O, C Prigent-Combaret, J Caballero-Mellado, and Y Moenne-Loccoz. 2009. “*Pseudomonas Fluorescens* and Closely-Related Fluorescent

- Pseudomonads as Biocontrol Agents of Soil-Borne Phytopathogens.” *Letters in Applied Microbiology* 48: 505–12. <https://doi.org/10.1111/j.1472-765X.2009.02566.x>.
- Cunnac, Sébastien, Magdalen Lindeberg, and Alan Collmer. 2009. “Pseudomonas Syringae Type III Secretion System Effectors: Repertoires in Search of Functions.” *Current Opinion in Microbiology* 12 (1): 53–60. <https://doi.org/10.1016/j.mib.2008.12.003>.
- Curto, Miguel, Emilio Camafeita, Juan A Lopez, and Ana M Maldonado. 2006. “A Proteomic Approach to Study Pea (*Pisum Sativum*) Responses to Powdery Mildew (*Erysiphe Pisi*).” *Proteomics* 6: S163–74. <https://doi.org/10.1002/pmic.200500396>.
- Danhorn, Thomas, and Clay Fuqua. 2007. “Biofilm Formation by Plant-Associated Bacteria.” *Annu Rev Microbiol.* 61: 401–22. <https://doi.org/10.1146/annurev.micro.61.080706.093316>.
- Davey, Mary Ellen, and George A O Toole. 2000. “Microbial Biofilms : From Ecology to Molecular Genetics.” *Microbiology Nad Molecualr Biology Reviews* 64 (4): 847–67.
- Defraia, Christopher T, Eric A Schmelz, and Zhonglin Mou. 2008. “A Rapid Biosensor-Based Method for Quantification of Free and Glucose-Conjugated Salicylic Acid.” *Plant Methods* 4 (28): 1–11. <https://doi.org/10.1186/1746-4811-4-28>.

- Dempsey, D'Maris, A Corina Vlot, Mary C Wildermuth, and Daniel F Klessig. 2011. "Salicylic Acid Biosynthesis and Metabolism." *The Arabidopsis Book* e0156: 1–24. <https://doi.org/10.1199/tab.0156>.
- Dong, Xinnian, Michael Mindrinos, R D Keith, and Frederick M Ausubel. 1991. "Induction of Arabidopsis Defense Genes by Virulent and Avirulent Pseudomonas Syringae Strains and by a Cloned Avirulence Gene." *The Plant Cell* 3: 61–72.
- Dow, J Maxwell, Lisa Crossman, Kim Findlay, Yong-qiang He, Jia-xun Feng, and Ji-liang Tang. 2003. "Biofilm Dispersal in Xanthomonas Campestris Is Controlled by Cell – Cell Signaling and Is Required for Full Virulence to Plants." *PNAS* 100 (19): 10995–0.
- Engl, Christoph, Christopher J Waite, Joseph F Mckenna, Mark H Bennett, Thorsten Hamann, and Martin Buck. 2014. "Chp8, a Diguanylate Cyclase from Pseudomonas Syringae Pv. Tomato DC3000, Suppresses the Pathogen-Associated Molecular Pattern Flagellin, Increases Extracellular Polysaccharides, and Promotes Plant Immune Evasion." *MBio* 5 (3): 1–11. <https://doi.org/10.1128/mBio.01168-14>.Editor.
- Espinosa-Urgel, Manuel, Roberto Kolter, and Juan-Luis Ramos. 2002. "Root Colonization by Pseudomonas Putida: Love at First Sight." *Microbiology* 148: 341–44.
- Fakhr, Mohamed K., Alejandro Peñaloza-Vázquez, Ananda M. Chakrabarty, and

- Carol L. Bender. 1999. "Regulation of Alginate Biosynthesis in *Pseudomonas Syringae* Pv. *Syringae*." *Journal of Bacteriology* 181 (11): 3478–85.
- Farias, Gabriela A, and Adela Olmedilla. 2019. "Visualization and Characterization of *Pseudomonas Syringae* Pv . Tomato DC3000 Pellicles." *Microbial Biotechnology* 12 (4): 688–702. <https://doi.org/10.1111/1751-7915.13385>.
- Faulkner, Christine, and Silke Robatzek. 2012. "Plants and Pathogens: Putting Infection Strategies and Defence Mechanisms on the Map." *Current Opinion in Plant Biology* 15 (6): 699–707. <https://doi.org/10.1016/j.pbi.2012.08.009>.
- Fett, William F, and Michael F Dunn. 1989. "Exopolysaccharides Produced by Phytopathogenic *Pseudomonas Syringae* Pathovars in Infected Leaves of Susceptible Hosts." *Plant Physiol.* 89: 5–9.
- Flemming, Hans-Curt, Jost Wingender, Ulrich Szewzyk, Peter Steinberg, Scott A. Rice, and Staffan Kjelleberg. 2016. "Biofilms : An Emergent Form of Bacterial Life." *Nature Reviews Microbiology* 14: 563–75. <https://doi.org/10.1038/nrmicro.2016.94>.
- Flemming, Hans Curt, and Jost Wingender. 2010. "The Biofilm Matrix." *Nature Reviews Microbiology* 8 (9): 623–33. <https://doi.org/10.1038/nrmicro2415>.
- Fouts, Derrick E, Robert B Abramovitch, James R Alfano, Angela M Baldo, C Robin Buell, Samuel Cartinhour, Arun K Chatterjee, et al. 2002. "Genomewide Identification of *Pseudomonas Syringae* Pv . Tomato DC3000

- Promoters Controlled by the HrpL Alternative Sigma Factor.” *PNAS* 99 (4): 2275–80.
- Franklin, Michael J, David E Nivens, Joel T Weadge, and Lynne Howell. 2011. “Biosynthesis of the *Pseudomonas Aeruginosa* Extracellular.” *Frontiers in Microbiology* 2: 1–16. <https://doi.org/10.3389/fmicb.2011.00167>.
- Fujishige, Nancy A, Neel N Kapadia, Peter L De Hoff, and Ann M Hirsch. 2006. “Investigations of *Rhizobium* Biofilm Formation.” *FEMS Microbiol Ecol* 56: 195–206. <https://doi.org/10.1111/j.1574-6941.2005.00044.x>.
- Geng, X., J. Cheng, A. Gangadharan, and D. Mackey. 2012. “The Coronatine Toxin of *Pseudomonas Syringae* Is a Multifunctional Suppressor of *Arabidopsis* Defense.” *The Plant Cell* 24 (11): 4763–74. <https://doi.org/10.1105/tpc.112.105312>.
- Georgiou, Christos D, Nikos Tairis, Anna Sotiropoulou, Christos D Georgiou, Nikos Tairis, and Anna Sotiropoulou Hydroxyl. 2000. “Hydroxyl Radical Scavengers Inhibit Lateral- Type Sclerotial Differentiation and Growth in Phytopathogenic Fungi.” *Mycologia* 92 (2): 825–34. <https://doi.org/10.1080/00275514.2000.12061226>.
- Glazebrook, Jane. 2005. “Contrasting Mechanisms of Defense against Biotrophic and Necrotrophic Pathogens.” *Annu. Rev. Phytopathol.* 43: 205–27. <https://doi.org/10.1146/annurev.phyto.43.040204.135923>.
- Godfrey, S, J Mansfield, D Corry, H Lovell, R Jackson, and D Arnold. 2010.

- “Confocal Imaging of *Pseudomonas Syringae* Pv . Phaseolicola Colony Development in Bean Reveals Reduced Multiplication of Strains Containing the Genomic Island PPHGI-1.” *MPMI* 23 (10): 1294–1302.
- Gómez-Gómez, Lourdes, and Thomas Boller. 2000. “FLS2: An LRR Receptor-like Kinase Involved in the Perception of the Bacterial Elicitor Flagellin in *Arabidopsis*.” *Molecular Cell* 5 (6): 1003–11. [https://doi.org/10.1016/S1097-2765\(00\)80265-8](https://doi.org/10.1016/S1097-2765(00)80265-8).
- Grasdalen, Hans. 1983. “High-Field, 1H-n.m.r. Spectroscopy of Alginate: Sequential Structure and Linkage Conformations.” *Carbohydrate Research* 118: 255–60.
- Gutknecht, John. 1990. “Salicylates and Proton Transport through Lipid Bilayer Membranes : A Model for Salicylate-Induced Uncoupling and Swelling in Mitochondria.” *J. Membrane Biol* 115: 253–60.
- Hay, Iain D, Zahid Ur Rehman, M Fata Moradali, Yajie Wang, and Bernd H A Rehm. 2013. “Microbial Alginate Production , Modification and Its Applications.” *Microbial Biotechnology* 6: 637–50. <https://doi.org/10.1111/1751-7915.12076>.
- Hengge, Regine. 2009. “Principles of C-Di-GMP Signalling in Bacteria.” *Nature Reviews Microbiology* 7: 263–73. <https://doi.org/10.1038/nrmicro2109>.
- Hoiby, Niels, Oana Ciofu, and Thomas Bjarnsholt. 2010. “*Pseudomonas Aeruginosa* Biofilms in Cystic Fibrosis.” *Future Microbiology* 5 (11): 1663–74.

- Ishiga, Takako, Yasuhiro Ishiga, Shigeyuki Betsuyaku, and Nobuhiko Nomura. 2018. "AlgU Contributes to the Virulence of *Pseudomonas Syringae* Pv . Tomato DC3000 by Regulating Production of the Phytotoxin Coronatine." *Journal of General Plant Pathology* 84: 189–201. <https://doi.org/10.1007/s10327-018-0775-6>.
- Ishiga, Yasuhiro, and Yuki Ichinose. 2016. "Pseudomonas Syringae Pv. Tomato OxyR Is Required for Virulence in Tomato and Arabidopsis." *MPMI* 29 (2): 119–31.
- Jelenska, Joanna, Sandra M. Davern, Robert F. Standaert, Saed Mirzadeh, and Jean T. Greenberg. 2017. "Flagellin Peptide Flg22 Gains Access to Long-Distance Trafficking in Arabidopsis via Its Receptor, FLS2." *Journal of Experimental Botany* 68 (7): 1769–83. <https://doi.org/10.1093/jxb/erx060>.
- Jia, Wensuo, and William John Davies. 2007. "Modification of Leaf Apoplastic PH in Relation to Stomatal Sensitivity to Root-Sourced Abscisic Acid Signals." *Plant Physiology* 143: 68–77. <https://doi.org/10.1104/pp.106.089110>.
- Jones, Jonathan D G, and Jeffery L. Dangl. 2006. "The Plant Immune System." *Nature* 444 (7117): 323–29. <https://doi.org/10.1038/nature05286>.
- Joo, Hwang-soo, and Michael Otto. 2012. "Review Molecular Basis of In Vivo Biofilm Formation by Bacterial Pathogens." *Chemistry & Biology* 19 (12): 1503–13. <https://doi.org/10.1016/j.chembiol.2012.10.022>.
- Jørgensen, T Glarborg, Ulla Sivertsen Weis-fogh, H H Nielsen, H P Olesen, T

Glarborg Jörgensen, Ulla Sivertsen Weis-fogh, and H H Nielsen. 1976.

“Salicylate- and Aspirin-Induced Uncoupling of Oxidative Phosphorylation in Mitochondria Isolated from the Mucosal Membrane of the Stomach.”

Scandinavian Journal of Clinical and Laboratory Investigation 36.

<https://doi.org/10.1080/00365517609054490>.

Kadota, Yasuhiro, Jan Sklenar, Paul Derbyshire, Lena Stransfeld, Shuta Asai,

Vardis Ntoukakis, Jonathan D G Jones, et al. 2014. “Direct Regulation of the NADPH Oxidase RBOHD by the PRR-Associated Kinase BIK1 during Plant Immunity.” *Molecular Cell* 54: 43–55.

<https://doi.org/10.1016/j.molcel.2014.02.021>.

Kang, Yaowei, Huanli Liu, Stéphane Genin, Mark A Schell, and Timothy P

Denny. 2002. “*Ralstonia Solanacearum* Requires Type 4 Pili to Adhere to Multiple Surfaces and for Natural Transformation and Virulence.” *Molecular Microbiology* 2: 427–37.

Katagiri, Fumiaki, Roger Thilmony, and Sheng Yang. 2002. “The *Arabidopsis*

Thaliana-*Pseudomonas Syringae*.” *The Arabidopsis Book* 1 (e0039): 1–35.

<https://doi.org/10.1199/tab.0039>.

Koczan, Jessica M, Molly J Mcgrath, Youfu Zhao, and George W Sundin. 2009.

“Contribution of *Erwinia Amylovora* Exopolysaccharides Amylovoran and Levan to Biofilm Formation : Implications in Pathogenicity.” *Phytopathology* 99 (11): 1237–44.

- Kragh, Kasper N, Jaime B Hutchison, Gavin Melaugh, Chris Rodesney, Aled E L Roberts, Yasuhiko Irie, Peter Ø Jensen, Stephen P Diggle, Rosalind J Allen, and Vernita Gordon. 2016. "Role of Multicellular Aggregates in Biofilm Formation." *MBio* 7 (2): 1–11. <https://doi.org/10.1128/mBio.00237-16>. Editor.
- Kubicek, Christian P., Trevor L. Starr, and N. Louise Glass. 2014. "Plant Cell Wall-Degrading Enzymes and Their Secretion in Plant-Pathogenic Fungi." *Annual Review of Phytopathology* 52 (1): 427–51. <https://doi.org/10.1146/annurev-phyto-102313-045831>.
- Kunze, Gernot, Cyril Zipfel, Silke Robatzek, Karsten Niehaus, Thomas Boller, and Georg Felix. 2004. "The N Terminus of Bacterial Elongation Factor Tu Elicits Innate Immunity in Arabidopsis Plants." *The Plant Cell* 16: 3496–3507. <https://doi.org/10.1105/tpc.104.026765>. Crude.
- Kus, Julianne V, Kasia Zaton, Raani Sarkar, and Robin K Cameron. 2002. "Age-Related Resistance in Arabidopsis Is a Developmentally Regulated Defense Response to *Pseudomonas Syringae*." *The Plant Cell* 14 (2): 479–90. <https://doi.org/10.1105/tpc.010481>. tions.
- Laue, Heike, Alexander Schenk, Hongqiao Li, Lotte Lambertsen, Thomas R. Neu, Søren Molin, and Matthias S. Ullrich. 2006. "Contribution of Alginate and Levan Production to Biofilm Formation by *Pseudomonas Syringae*." *Microbiology* 152 (10): 2909–18. <https://doi.org/10.1099/mic.0.28875-0>.
- Li, Qiang, Anhua Hu, Jingjing Qi, Wanfu Dou, Xiujuan Qin, and Xiuping Zou.

2020. "CsWAKL08, a Pathogen-Induced Wall-Associated Receptor-like Kinase in Sweet Orange , Confers Resistance to Citrus Bacterial Canker via ROS Control and JA Signaling." *Horticulture Research* 7 (42): 1–15.
<https://doi.org/10.1038/s41438-020-0263-y>.
- Mann, Ethan E, and Daniel J Wozniak. 2012. "Pseudomonas Biofilm Matrix Composition and Niche Biology." *FEMS Microbiol Rev.* 36 (4): 893–916.
<https://doi.org/10.1111/j.1574-6976.2011.00322.x.Pseudomonas>.
- Markel, Eric, Hollie Dalenberg, Caroline L Monteil, Boris A Vinatzer, and Bryan Swingle. 2018. "An AlgU-Regulated Antisense Transcript Encoded within the Pseudomonas Syringae FleQ Gene Has a Positive Effect on Motility." *Journal of Bacteriology* 200 (7): 1–16.
- Markel, Eric, Paul Stodghill, Zhongmeng Bao, Christopher R Myers, and Bryan Swingle. 2016. "AlgU Controls Expression of Virulence Genes in Pseudomonas Syringae Pv . Tomato DC3000" 198 (17): 2330–44.
<https://doi.org/10.1128/JB.00276-16.Editor>.
- Mitra, Prajakta Pradhan, and Dominique Loqué. 2014. "Histochemical Staining of Arabidopsis Thaliana Secondary Cell Wall Elements." *Journal of Visualized Experiments* 87 (e51381): 1–11. <https://doi.org/10.3791/51381>.
- Mohan, Rajinikanth, Marie Benton, Emily Dangelmaier, Zhengqing Fu, and Akila Chandra Sekhar. 2018. "Quorum Sensing and Biofilm Formation in Pathogenic and Mutualistic Plant-Bacterial Interactions." *Implication of*

Quorum Sensing System in Biofilm Formation and Virulence, 133–60.

<https://doi.org/10.1007/978-981-13-2429-1>.

Monier, J, and S E Lindow. 2004. “Frequency , Size , and Localization of Bacterial Aggregates on Bean Leaf Surfaces.” *Applied and Environmental Microbiology* 70 (1): 346–55. <https://doi.org/10.1128/AEM.70.1.346>.

Muhammadi, and Nuzhat Ahmed. 2007. “Genetics of Bacterial Alginate: Alginate Genes Distribution, Organization and Biosynthesis in Bacteria.” *Current Genomics* 8 (3): 191–202. <https://doi.org/10.2174/138920207780833810>.

Nobori, Tatsuya, André C Velásquez, Jingni Wu, Brian H Kvitko, James M Kremer, and Yiming Wang. 2018. “Transcriptome Landscape of a Bacterial Pathogen under Plant Immunity.” *PNAS* 115 (3): E3055–64. <https://doi.org/10.1073/pnas.1800529115>.

Norman, Christel, Katharine A Howell, A Harvey Millar, James M Whelan, and David A Day. 2004. “Salicylic Acid Is an Uncoupler and Inhibitor of Mitochondrial Electron Transport.” *Plant Physiology* 134: 492–501. <https://doi.org/10.1104/pp.103.031039.been>.

O’Leary, Brendan M, Arantza Rico, Sarah Mccraw, Helen N Fones, and Gail M Preston. 2014. “The Infiltration-Centrifugation Technique for Extraction of Apoplastic Fluid from Plant Leaves Using *Phaseolus Vulgaris* as an Example.” *Journal of Visualized Experiments* 94 (e52113): 1–8. <https://doi.org/10.3791/52113>.

- Ortiz-martín, Inmaculada, Richard Thwaites, Alberto P Macho, John W Mansfield, and Carmen R Beuzón. 2010. "Positive Regulation of the Hrp Type III Secretion System in *Pseudomonas Syringae* Pv . *Phaseolicola*." *MPMI* 23 (5): 665–81.
- Osman, S F, W F Fett, Eastern Regional, M Gross, W F Fett, Plant Pathogenic Bacteria, and Hatching Green. 1986. "Exopolysaccharides of the Phytopathogen *Pseudomonas Syringae* Pv . *Glycinea*." *Journal of Bacteriology* 166 (1): 66–71.
- Ozenbergert, Bradley A, Timothy J Brickman, and Mark A Mcintosh. 1989. "Nucleotide Sequence of *Escherichia Coli* Isochorismate Synthetase Gene EntC and Evolutionary Relationship of Isochorismate Synthetase and Other Chorismate-Utilizing Enzymes." *Journal of Bacteriology* 171 (2): 775–83.
- Palmer, Ian Arthur, Zhenhua Shang, and Zheng Qing Fu. 2017. "Salicylic Acid-Mediated Plant Defense : Recent Developments , Missing Links , and Future Outlook." *Front. Biol* 12 (4): 258–70. <https://doi.org/10.1007/s11515-017-1460-4>.
- Peñaloza-Vázquez, Alejandro, Saranga P Kidambi, Ananda M Chakrabarty, Alejandro Pen, and Carol L Bender. 1997. "Characterization of the Alginate Biosynthetic Gene Cluster in *Pseudomonas Syringae* Pv . *Syringae*." *Journal of Bacteriology* 179 (14): 4464–72.
- Pérez-mendoza, Daniel, Antonia Felipe, María Dolores Ferreiro, and Juan

- Sanjuán. 2019. “AmrZ and FleQ Co-Regulate Cellulose Production in *Pseudomonas Syringae* Pv . Tomato DC3000.” *Frontier in Microbiology* 10: 1–16. <https://doi.org/10.3389/fmicb.2019.00746>.
- Prada-ramírez, Harold A, Daniel Pérez-mendoza, Antonia Felipe, Francisco Martínez-granero, Rafael Rivilla, Juan Sanjuán, and María-trinidad Gallegos. 2016. “AmrZ Regulates Cellulose Production in *Pseudomonas Syringae* Pv . Tomato DC3000.” *Molecular Microbiology* 99 (5): 960–77. <https://doi.org/10.1111/mmi.13278>.
- Prithviraj, B, H P Bais, T Weir, B Suresh, E H Najarro, B V Dayakar, H P Schweizer, and J M Vivanco. 2005. “Down Regulation of Virulence Factors of *Pseudomonas Aeruginosa* by Salicylic Acid Attenuates Its Virulence on *Arabidopsis Thaliana* and *Caenorhabditis Elegans*.” *Infection and Immunity* 73 (9): 5319–28. <https://doi.org/10.1128/IAI.73.9.5319>.
- Prithviraj, B, T Weir, H P Bais, H P Schweizer, and J M Vivanco. 2005. “Microreview Plant Models for Animal Pathogenesis.” *Cellular Microbiology* 7 (3): 315–24. <https://doi.org/10.1111/j.1462-5822.2005.00494.x>.
- Quiñones, Beatriz, Glenn Dulla, and Steven E Lindow. 2005. “Exopolysaccharide Production , Motility , and Virulence in *Pseudomonas Syringae*.” *MPMI* 18 (7): 682–93.
- Quiñones, Beatriz, Catherine J Pujol, and Steven E Lindow. 2004. “Regulation of AHL Production and Its Contribution to Epiphytic Fitness in *Pseudomonas*

Syringae.” *MPMI* 17 (5): 521–31.

Rasamiravaka, Tsiry, Quentin Labtani, Pierre Duez, and Mondher El Jaziri Jaziri. 2015. “The Formation of Biofilms by *Pseudomonas Aeruginosa* : A Review of the Natural and Synthetic Compounds Interfering with Control Mechanisms.” *BioMed Research International* 2015 (759348): 1–17.
<http://dx.doi.org/10.1155/2015/759348>.

Renzi, Marsilio, Angelo Mazzaglia, and Giorgio Mariano Balestra. 2012. “Widespread Distribution of Kiwifruit Bacterial Canker Caused by the European *Pseudomonas Syringae* Pv. *Actinidiae* Genotype in the Main Production Areas of Portugal.” *Phytopathologia Mediterranea* 51 (2): 402–9.

Sinha, Alok Krishna, Monika Jaggi, Badmi Raghuram, and Narendra Tuteja. 2011. “Mitogen-Activated Protein Kinase Signaling in Plants under Abiotic Stress.” *Plant Signaling & Behavior* 6 (2): 196–203.
<https://doi.org/10.4161/psb.6.2.14701>.

Strathmann, Martin, Jost Wingender, and Hans-curt Flemming. 2002. “Application of Fluorescently Labelled Lectins for the Visualization and Biochemical Characterization of Polysaccharides in Biofilms of *Pseudomonas Aeruginosa*.” *Journal of Microbiological Method* 50: 237–48.

Subramoni, Sujatha, Naeem Nathoo, Eugene Klimov, Ze-chun Yuan, Tina Britta Jordan, and Eberhard Karls. 2014. “*Agrobacterium Tumefaciens* Responses to Plant-Derived Signaling Molecules.” *Frontiers in Plant Science* 5: 1–12.

<https://doi.org/10.3389/fpls.2014.00322>.

Taj, Gohar, Payal Agarwal, Murray Grant, and Anil Kumar. 2010. "MAPK Machinery in Plants." *Plant Signaling & Behavior* 5 (11): 1370–78.
<https://doi.org/10.4161/psb.5.11.13020>.

Torrens-spence, Michael P, Anastassia Bobokalonova, Valentina Carballo, Amber Shen, Jing-ke Weng, and Christopher M Glinkerman. 2019. "PBS3 and EPS1 Complete Salicylic Acid Biosynthesis from Isochorismate in Arabidopsis." *Molecular Plant* 12: 1577–86.
<https://doi.org/10.1016/j.molp.2019.11.005>.

Tsuda, Kenichi, Masanao Sato, Jane Glazebrook, Jerry D Cohen, Fumiaki Katagiri, St Paul, and St Paul. 2008. "Interplay between MAMP-Triggered and SA-Mediated Defense Responses." *The Plant Journal* 52: 763–75.
<https://doi.org/10.1111/j.1365-313X.2007.03369.x>.

Ude, Susanne, Dawn L Arnold, Christina D Moon, Tracey Timms-wilson, and Andrew J Spiers. 2006. "Biofilm Formation and Cellulose Expression among Diverse Environmental Pseudomonas Isolates." *Environmental Microbiology* 8 (11): 1997–2011. <https://doi.org/10.1111/j.1462-2920.2006.01080.x>.

Uquillas, Carolina, Ingrid Letelier, Francisca Blanco, Xavier Jordana, and Loreto Holuigue. 2004. "NPR1-Independent Activation of Immediate Early Salicylic Acid-Responsive Genes in Arabidopsis." *Molecular Plant-Microbe Interactions* 17 (1): 34–42. <https://doi.org/10.1094/MPMI.2004.17.1.34>.

- Vargas, Paola, Gabriela A Farias, Joaquina Nogales, Harold Prada, Vivian Carvajal, Matilde Barón, Rafael Rivilla, Marta Martín, Adela Olmedilla, and María-trinidad Gallegos. 2013. "Plant Flavonoids Target *Pseudomonas Syringae* Pv . Tomato DC3000 Flagella and Type III Secretion System." *Environmental Microbiology Reports* 5 (6): 841–50.
<https://doi.org/10.1111/1758-2229.12086>.
- Varvaro, L., R. Fanigliulo, and N. M. Babelegoto. 1993. "Transmission Electron Microscopy of Susceptible and Resistant Tomato Leaves Following Infection with *Pseudomonas Syringae* Pv. Tomato." *Journal of Phytopathology* 138 (4): 265–73. <https://doi.org/10.1111/j.1439-0434.1993.tb01386.x>.
- Visnapuu, Triinu, Karin Mardo, Cristina Mosoarca, Alina D Zamfir, Armands Vigants, and Tiina Alamäe. 2011. "Levansucrases from *Pseudomonas Syringae* Pv . Tomato and P . Chlororaphis Subsp . Aurantiaca : Substrate Specificity , Polymerizing Properties and Usage of Different Acceptors for Fructosylation." *Journal of Biotechnology* 155 (3): 338–49.
<https://doi.org/10.1016/j.jbiotec.2011.07.026>.
- Wang, Li, Seiko Makino, Ashim Subedee, and Adam J Bogdanove. 2007. "Novel Candidate Virulence Factors in Rice Pathogen *Xanthomonas Oryzae* Pv . *Oryzicola* as Revealed by Mutational Analysis." *Applied and Environmental Microbiology* 73 (24): 8023–27. <https://doi.org/10.1128/AEM.01414-07>.
- Whalen, Maureen C, Roger W Innes, Andrew F Bent, and Brian J Staskawicz. 1991. "Identification of *Pseudomonas Syringae* Pathogens of Arabidopsis

and a Bacterial Locus Determining Avirulence on Both Arabidopsis and Soybean.” *The Plant Cell* 3: 49–59.

Wilson, Daniel C., Christine J. Kempthorne, Philip Carella, David K. Liscombe, and Robin K. Cameron. 2017. “Age-Related Resistance in *Arabidopsis Thaliana* Involves the MADS-Domain Transcription Factor SHORT VEGETATIVE PHASE and Direct Action of Salicylic Acid on *Pseudomonas Syringae*.” *Molecular Plant-Microbe Interactions* 30 (11): 919–29. <https://doi.org/10.1094/MPMI-07-17-0172-R>.

Xin, Xiu-fang, and Sheng Yang He. 2013. “DC3000 : A Model Pathogen for Probing Disease Susceptibility and Hormone Signaling in Plants.” *Annu. Rev. Phytopathol.* 51: 473–98. <https://doi.org/10.1146/annurev-phyto-082712-102321>.

Yang, Liang, Morten Theil Rybtke, Tim Holm Jakobsen, Morten Hentzer, Thomas Bjarnsholt, Michael Givskov, and Tim Tolker-nielsen. 2009. “Computer-Aided Identification of Recognized Drugs as *Pseudomonas Aeruginosa* Quorum-Sensing Inhibitors.” *Antimicrobial Agent and Chemotherapy* 53 (6): 2432–43. <https://doi.org/10.1128/AAC.01283-08>.

Yu, Jing, Alejandro Penaloza-Vázquez, Ananda M. Chakrabarty, and Carol L. Bender. 1999. “Involvement of the Exopolysaccharide Alginate in the Virulence and Epiphytic Fitness of *Pseudomonas Syringae* Pv. *Syringae*.” *Molecular Microbiology* 33 (4): 712–20. <https://doi.org/10.1046/j.1365-2958.1999.01516.x>.

- Yuan, Jing, and Sheng Yang He. 1996. "The *Pseudomonas Syringae* Hrp Regulation and Secretion System Controls the Production and Secretion of Multiple Extracellular Proteins." *Journal of Bacteriology* 178 (21): 6399–6402.
- Zhang, Jie, and Jian Min Zhou. 2010. "Plant Immunity Triggered by Microbial Molecular Signatures." *Molecular Plant* 3 (5): 783–93.
<https://doi.org/10.1093/mp/ssq035>.
- Zheng, Xiao-yu, Mian Zhou, Heejin Yoo, Jose L. Pruneda-Paz, Natalie Weaver Spivey, Steve A. Kay, and Xinnian Dong. 2015. "Spatial and Temporal Regulation of Biosynthesis of the Plant Immune Signal Salicylic Acid." *Proceedings of the National Academy of Sciences* 112 (30): 9166–73.
<https://doi.org/10.1073/pnas.1511182112>.
- Zheng, Xiao Yu, Natalie Weaver Spivey, Weiqing Zeng, Po Pu Liu, Zheng Qing Fu, Daniel F. Klessig, Sheng Yang He, and Xinnian Dong. 2012. "Coronatine Promotes *Pseudomonas Syringae* Virulence in Plants by Activating a Signaling Cascade That Inhibits Salicylic Acid Accumulation." *Cell Host and Microbe* 11 (6): 587–96. <https://doi.org/10.1016/j.chom.2012.04.014>.
- Zipfel, Cyril. 2009. "Early Molecular Events in PAMP-Triggered Immunity." *Current Opinion in Plant Biology* 12 (4): 414–20.
<https://doi.org/10.1016/j.pbi.2009.06.003>.